

Investigation of Possible Hydrogen Shielding Effect on Epithermal Neutron Activation Analysis

--A computation and experimental
approach

Yang “Alex” Zhou

Adviser: Dr. Erich Schneider
Dr. Sheldon Landsberger

University of Texas at Austin
May 6, 2010

Introduction

Neutron activation is a popular analytical technique used to determine the presence and concentration of certain elements. It has several variations, including thermal neutron, epithermal neutron, fast neutron activation, etc, for different applications; all of those variations are non-destructive, and sensitive to small quantity. While trying to determine the concentration of Cl and Br in the light water solution, Dr. Landsberger's team found the epithermal neutron activation analysis results were 25% lower than the conventional chemical method. They were not able to determine the cause of such discrepancy. This study was motivated to re-examine such discrepancy, and to study its possible causes. Furthermore, the study tries to determine if such discrepancy, if it exists, was linked with thermal neutron cut off or hydrogen absorption of neutrons.

A computer simulation using the Monte Carlo radiation transport software MCNPX was developed to radiate sample Cl & Br solutions of known mass concentrations in a simulated TRIGA reactor core at 500 KW steady state power. [1] The neutron activation rate of Br, Cl at each concentration was then calculated. Such procedure was then repeated for heavy water solutions. Finally, a cadmium shield was added to eliminate thermal neutrons; all samples were tested again using epithermal neutron activation. The actual neutron activation experiment was also carried out in the University of Texas's TRIGA Mark II reactor. A total of 40 samples of Br & Cl solution (with and without Cd, in light water and in heavy water) were irradiated in the reactor at 500 KW steady state power.

Background and Theory

Neutron activation analysis utilizes a neutron source to bombard targeted elements with neutron flux; once such element absorbs a neutron, it is activated to an isotope of the same element—its proton number remains unchanged—which is usually radioactive. Those activation products then would decay with specific gamma emissions. By studying their emission spectra, one can identify the presence of elements by matching characteristic peaks, and estimate element concentration through counting the number of emissions. [2]

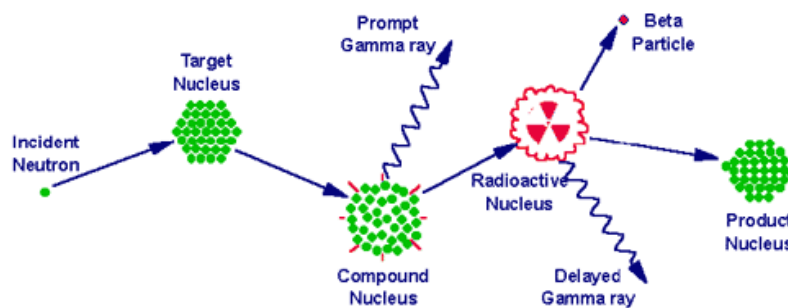


Figure 1, illustration of neutron activation reaction, the (n, γ) reaction

http://archaeometry.missouri.edu/naa_overview.html

The neutrons used for neutron activation analysis usually have low kinetic energies, and are classified as thermal neutron (~1eV) and epithermal neutron (1eV~1MeV) for the higher neutron cross-section at those energy levels. As one can observe from figures 2~3 below, in the thermal neutron region from 0 to about 1 eV, all Cl, Br, and Cd have a high thermal neutron cross-section; in the epithermal region from 1eV to 1MeV, their cross sections go down and exhibit much resonance before they finally enter the fast neutron region with low cross-sections.

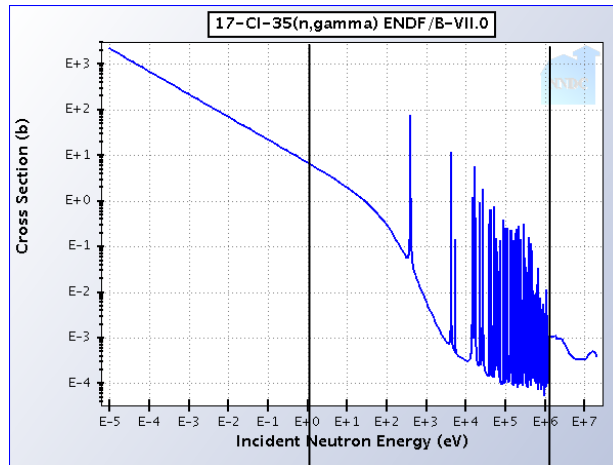


Figure 2, neutron activation cross-section spectrum for chlorine-35

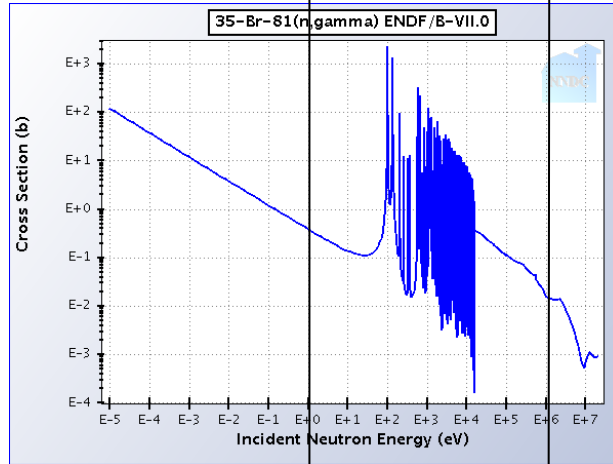


Figure 3, neutron activation cross-section spectrum for bromine-81

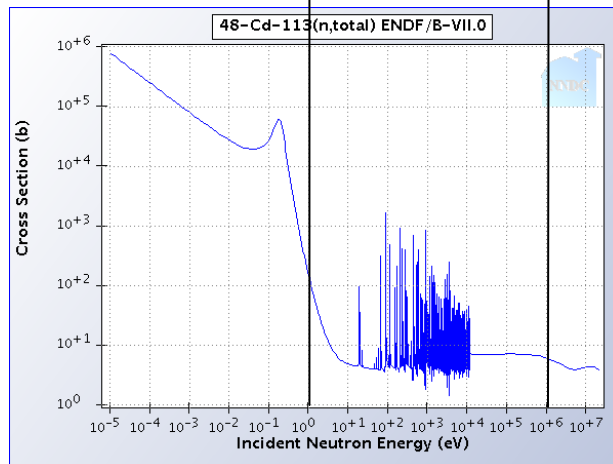


Figure 4, neutron activation cross-section spectrum for cadmium-113

Note the lines separate neutron cross sections in all three figures into thermal neutron and epithermal neutron regions. Also note the activation cross section of Br is about 1 order magnitude lower than that of Cl cross thermal and epithermal region.

This contrast between thermal neutron and epithermal neutron cross section is especially visible in cadmium, as seen in figure 4, with its thermal neutron cross section about 3 orders magnitude higher than those of Cl and Br; in epithermal neutron region, Cd's cross-section drops to about the same level as Cl and Br.

Because of the interfering interactions with other elements in the thermal neutron region, epithermal neutrons are sometimes preferred for select-irradiation to enhance the desired activation rate of targeting elements. [3], [4] In this case, cadmium shielding is usually used to eliminate thermal neutron from the volume containing the testing specimen due to cadmium's very high thermal neutron cross sections

Various causes for inaccuracy in (thermal and epithermal) neutron activation analysis have been reported, such as spectrum peak area distortion, interfering isotopes, the irregular shape of epithermal neutron distribution in the reactor, and hydrogen shielding. [4], [5], [6], [7] However, spectrum peak area distortion and irregular epithermal neutron distribution from the reactor are unlikely in the well-calibrated neutron activation facility at UT TRIGA reactor, as corrections for these had been applied. Interfering isotopic activation due to higher energy neutron should also be minimal in the epithermal neutron activation experiment. [6], [7], [8], [9]

Given the abundance of hydrogen in the sample and its large neutron cross section, hydrogen shielding appeared to be possible. As shown in figure 5 and 6, the total cross sections for hydrogen in thermal and epithermal neutron region is comparable if not higher than the cross sections for Cl and Br. The neutron cross section of

deuterium, on the other hand, is roughly one order of magnitude lower across the same energy spectrum.

This study compares simulated activation rates of Cl and Br in both light water and heavy water solutions at 5 different concentrations (0.001%, 0.01%, 0.1%, 1%, 10%). Experiments were also conducted to verify the computational results. These results would determine if hydrogen shielding indeed was responsible for the aberrant experimental result in the epithermal neutron activation analysis.

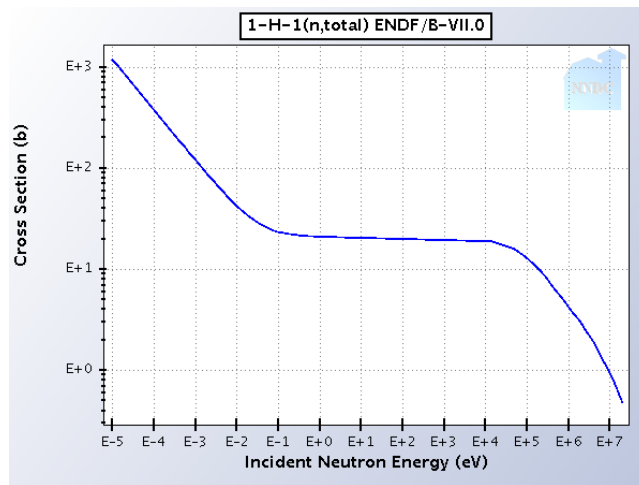


Figure 5, total neutron cross section spectrum for hydrogen.

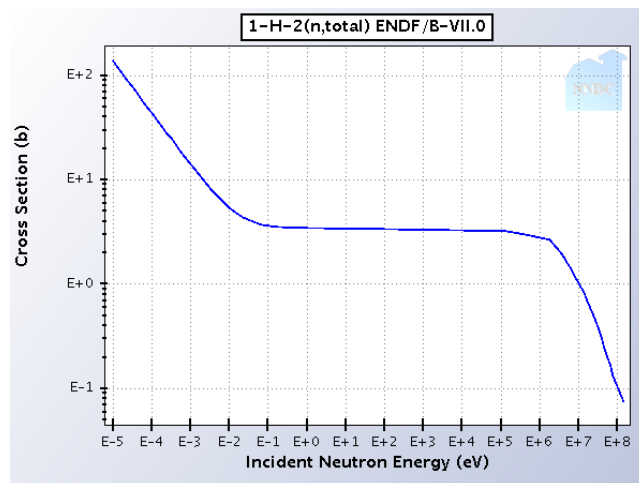


Figure 6, total neutron cross section spectrum for Deuterium.

Computer Simulation Methodology

To simulate the radiation field in the UT TRIGA reactor, the Monte Carlo radiation transport software MCNPX code was used. [1] An existing deck developed by Braisted provided the base model of the geometry and material compositions for the UT TRIGA reactor. [10] Figures 7 and 8 below show the geometric structure of the deck as plotted in the MCNP visual editor. The modeled reactor core is a 1.5 m tall, 1.4 m diameter cylinder submerged in water (pink areas in the figure). The U-Zr-H fuel pins (light blue tall cylinders) are arranged in a hexagonal cell lattice in the center of the reactor core, with four control rods (three orange and one purple cylinder) situated in the middle. The testing sample will be loaded in the reactor for neutron activation at spots indicated by the arrows in figures 7 and 8.

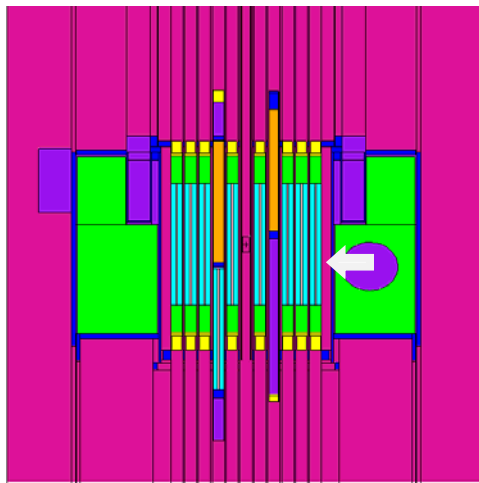


Figure 7, Side view of the UT TRIGA reactor from the existing MCNPX deck. Note, the arrow is pointed at the sample location in the reactor.

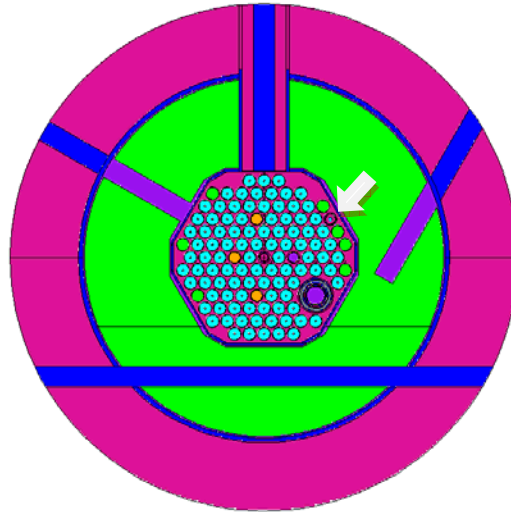


Figure 8, Top view of the UT TRIGA reactor from the existing MCNPX deck. Note, the arrow is pointed at the sample location in the reactor.

The radiation level of the TRIGA reactor was estimated using the criticality calculation feature of MCNPX. This so-called K-code calculation obtains the multiplication factor K_{eff} by tracking 10000 neutrons per generation for 60 generations. The initial guess for K_{eff} is set to 1.0; the results of the neutrons and the K_{eff} of the first 30 generations are discarded as the fission source must converge to its fundamental eigenmode. For better statistical results of the sample region in the much larger reactor core, more tracking particles and generations would be preferred. However, excessive computational resources would be required that way. The simulation of 10,000 particles and 60 generations took 20 minutes per run on an Intel Pentium 4 HT 3.00GHz computer.

Upon first execution, the K-code calculation revealed a slightly supercritical system with $K_{eff}=1.02\sim1.03$. The TRIGA model was then modified to lower the four control rods each by about 10 cm to reach criticality. Subsequent K-code calculation showed a critical system with $K_{eff} = 1.000 \pm 0.001$.

Because the MCNPX simulation generates the neutron flux distribution of a steady state reactor at random power level, the actual neutron flux of TRIGA reactor at 500 KW

steady state has to be calculated using a power scale factor. To determine the power scale factor, the power output of the simulated critical system was estimated with two MCNPX building tallies F4 and F7. Using F4 tally option 2, which tracked fission neutron flux, the average fission rate density of a single fuel pin was found to be 1.045E-3 fissions per cubic centimeter per second. The volume of each fuel pin was found to be 384.96 cm³ and the reactor core holds 98 fuel pins.

$$\begin{aligned} \text{Average fission rate} &= 1.045 \text{ e} - 3 \text{ fissions} / \text{sec.} \cdot \text{cm}^3 * 384.96 \text{ cm}^3 * 98 \text{ fuel pins} \\ &= 39.42 \text{ fissions} / \text{sec} \end{aligned}$$

$$\begin{aligned} \text{Average fission energy output} \\ &= 39.42 \text{ fissions/sec} * 200 \text{ MeV} / \text{fission} * 1.602 \text{ e} - 13 \text{ J} / \text{MeV} \\ &= 1.3 \text{ e} - 9 \text{ W} \end{aligned}$$

This number was double-checked by using F7 tally, which tracked average fission energy deposition of each fuel cell. Since samples would be irradiated at a steady state power of 500 Kilowatts, a multiplier was calculated.

$$\text{Energy Scale factor} = 500,000 \text{ W} / 1.3 \text{ e} - 9 \text{ W} = 4.345 \text{ e} 14$$

This multiplier would be used to adjust the results of all subsequent MCNPX tallies so that they corresponded to the radiation field intensity at 500 kW of fission power.

The samples, which consisted of chlorine and bromine solution of differing concentration in a polyethylene vial in each trial, were then developed using MCNPX. The cylindrical vial is 1.6 cm tall, 0.5 cm ID, 0.55 cm OD. Inside, NaCl and NaBr solution of 0.001%, 0.01%, 0.1%, 1%, and 10% in both water and heavy water (D₂O) were prepared. They were loaded in the sample holder as marked in figures 7, 8 and 9.

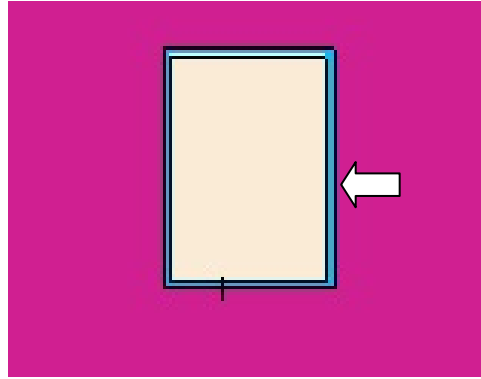


Figure 9, the polyethylene vial (the thin blue layer indicated by the arrow) is emerged in water. It held desired testing material chlorine and bromine solutions of different concentrations inside.

The neutron activation rate of each specimen was obtained using an F4 tally and scaled up with power scale factor and element number density. See table A in Appendix for the calculation and the complete list of number density values for various elements in different specimen. The resulting activation rate density of samples was in units of $\#/cm^3/sec$. Furthermore, the activation rate was assessed within two different energy bands: $< \sim 1$ eV for thermal neutrons, and 1eV-1MeV for epithermal/fast neutrons with the energy tally F.

The preliminary results had uncertainties of 40% when 10,000 neutron particles per generation were tracked. It appeared to be that 10,000 neutron particles could not provide a sufficient number of neutrons for a relatively small sample region in the reactor. In order to decrease the uncertainty to an acceptable level ($< 10\%$ in most cases), the number of particles tracked was increased to 1,000,000, which would be expected to decrease the uncertainty from 40% to 4%. However, the computational time for a single run of the MCNPX code then became close to 3 days. Therefore, a surface source substitution method by Wilson and Schneider was used to reduce computational requirements, as seen in figure 4. [11]



Figure 10, the surface source substitution method developed by Wilson and Schneider. Note the dash-lined circle as the surface source.

A three plane surface (one cylindrical surface, one top, and one bottom planes) surrounding the vial of specimen in the sample location is developed. As one can see in figures 11 and 12, the surface source that encloses the testing specimen was much smaller than the whole TRIGA reactor. An MCNPX SSW command was used to record the neutron flux through those surfaces that eventually entered the sample. After an initial run, a surface source file recording all neutron influx was generated and was then renamed as rssa for subsequent use. A new MCNPX source file was also developed to take advantage of the rssa surface source. Geometrically, the deck now only included the surface source, and the vials and samples inside, as seen in figure 13. An SSR command was used to recall the rssa file for the surface source configuration. F4 tallies with various multipliers were once again used to estimate the activation rates. Now only the initial run used the original code with full TRIGA reactor deck, which took about 3 days; all the subsequent simulation took much less computation time (less than 20 sec. each).

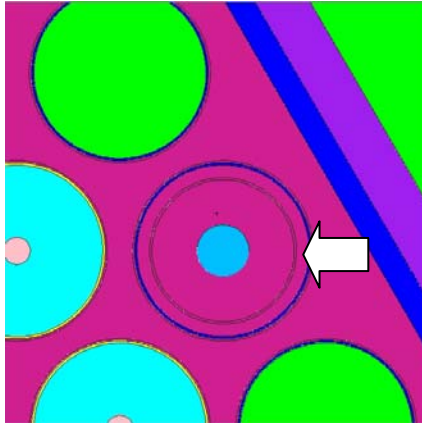


Figure 11, the close up of the sample holder location; note the thin layer indicated by the arrow is the surface source in the original deck.

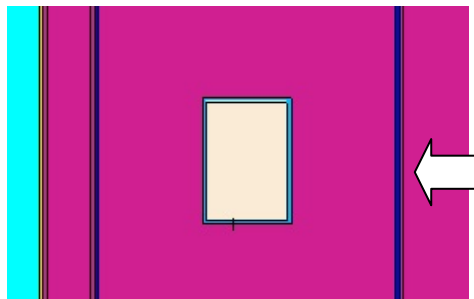


Figure 12, the side view of the sample holder location, note the thin layer indicated by the arrow is the surface source in the original deck.

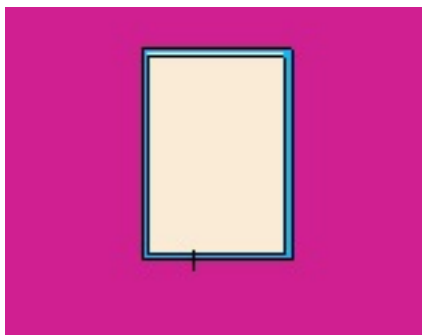


Figure 13, the new MCNPX code with only the surface source, the vial and samples. Note, the empty space outside the purple water is the outer boundary of this deck.

Using the new surface source, the activation rate of Cl, Br, H, D from NaCl and NaBr solution of 0.001%, 0.01%, 0.1%, 1%, and 10% in both water and heavy water (D_2O) were calculated. Finally, the rate was calculated again for all specimens with a Cd foil of 1mm thickness wrapped tightly around the polyethylene vial. Once again, the activation rate was broken into two energy levels of <1 eV for thermal neutron, and 1 eV~1 MeV for epithermal neutrons.

Neutron Activation Procedures and Calculation

The light water and heavy water solution of NaCl, NaBr were prepared using 100ml flasks, NaCl, NaBr salt, deionized light water and heavy water. **10.7 gram** of NaCl (10% of NaCl light water solution has a density of 1.07g/ml) was weighed and dissolved in deionized light water in a 100 ml flask. Light water was added until the solution reached 100 ml mark. 10 ml of the newly made 10% NaCl light water solution was transferred to a new 100 ml flask and refilled with light water until the solution reached 100 ml mark. The 1% NaCl light water solution was then made. In a similar fashion, the 0.1%, 0.01% and 0.001% NaCl light water solutions were made. NaBr light water solutions at different concentrations were also made in the same fashion. Note the density of 10% NaBr light water solution was also about 1.07 g/ml. **11.7 grams** of NaCl (density of 10% NaCl heavy water solution is 1.17g/ml) was weighed and dissolved in deionized heavy water in a 100 ml flask. Adding heavy water was continued until the solution reached 100 ml mark to make 10% NaCl heavy water solution. The above process was repeated until all 1%, 0.1%, 0.01% and 0.001% mass concentration solutions were made. The process was repeated again to make NaBr heavy water solution at the above mentioned five concentrations.

Due to the available reactor time, only 20 NaCl samples in light water and heavy water were tested in thermal and epithermal neutron activation tests.

After the sample solutions were prepared at the required mass concentration, they were then transferred into polyethylene vials. The vials were filled halfway, and then placed near the core of the reactor using the pneumatic system. The samples were irradiated at 500 KW steady state for 10sec~10 minutes depending on the mass concentration. The pneumatic system then pulled them out of the core; the samples were weighed and transferred into a new polyethylene vial to avoid the background interference of activated elements in the vial itself. The gamma emissions due to the decay of Cl-35 were counted using High Purity Germanium gamma ray detectors. The gamma spectrum was then produced as seen in figure 14. The peaks of gamma emission for Cl-35 was observed at 1642 kev; the area under the peak, as seen in the lower window of figure 14, was given enough count time to reach 5000 count to reduce uncertainties. The dead time was kept under 5% during the counting process.

Based on the measurement of the activity, count time, decay time, setup, geometry, and detection efficiency, software then applied several corrections for each sample, and calculated the mass concentration of targeted elements in the sample. Note, two standard reference material of tomato leaves (SRM 1573a, 6600 ppm Cl) were irradiated with and without cadmium coating each for 1 min at 500 KW steady state.

The activation rate of the element and its concentration are related as:

$$N_{(A+1)} = \frac{\Phi \sigma_{ad} N_{oA}}{\lambda_{(A+1)}} \left[1 - e^{-\lambda_{(A+1)} t_R} \right] e^{-\lambda_{(A+1)} t}$$

where $N_{(A+1)}$ is the atomic number density of activated isotope (activation rate if we normalized by 1 sec. of irradiation time); σ_{ad} is the neutron absorption cross section of the original isotope, N_{oA} is the number density of the original isotope, t_R is the irradiation

time (1 sec. in our simulation), t is the time after irradiation, and $\lambda_{(A+1)}$ is the decay constant of the activated isotope. [12] [13] [14] Assuming irradiation time is 1 sec, time after irradiation is short and the half-life is relatively long. The concentration of the element in the sample can be calculated as:

$$N_{ad} = \frac{N_{(A+1)} \lambda_{(A-1)}}{\sigma_{ad} \phi}$$

Oftentimes, the mass concentration of the elements was established using the relative method. The sample and a standard reference of known material concentration were irradiated together in the reactor. By comparing the gamma emission of the activated product, the concentration of the sample can be easily determined. [13] The simple calculation can be carried out as:

$$C_{\text{sample}} = C_{\text{std ref}} \frac{W_{\text{std}}}{W_{\text{sample}}} \frac{A_{\text{sample}}}{A_{\text{std}}}$$

where C is the element concentration, W is element weight and A is element activity. In addition, the use of standard reference material provides correction coefficients for the reactor configuration, geometry, and detector efficiency for the calculation. [14] [15]



Figure 14, gamma spectrum of neutron activation analysis

<http://reactor.engr.wisc.edu/naa/moreNAA.htm>

Data Analysis

Computer Simulation

The total activation (capture) rate density of Cl, Br, H, D and their uncertainties from the simulation are obtained from the F4 tally output file and scaled as described above. The activation rate per atom (probability of activation per atom) is calculated by dividing the total activation rate density by number density of respective elements. See Table B in Appendix for complete list of values. Note, all the activation rates are normalized by 1 sec. irradiation time.

For the neutron activation rate of Cl without cadmium shield, figure 15 showed that the epithermal neutron and total activation rate of Cl were identical in light water and heavy water. In both light water and heavy water samples, the epithermal neutron activation rate was about two orders of magnitude lower than the thermal (and total) neutron activation rate. The epithermal neutron and total activation rate of hydrogen in light water is about three orders of magnitude higher than deuterium in heavy water.

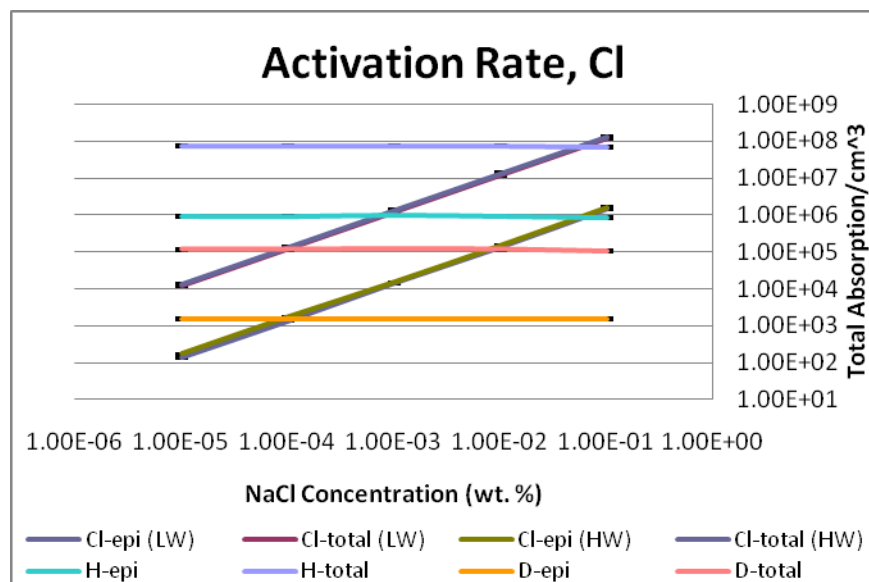


Figure 15, neutron activation rate of Cl in light water and heavy water

For neutron activation rate of Br without cadmium shield in figure 16, similar results were observed. From there, it was concluded that the Cl and Br activation rates were linear (in the lognormal graph) in their concentration in the solution, implying that even at high concentrations the salts did not induce a significant perturbation to the local radiation field.

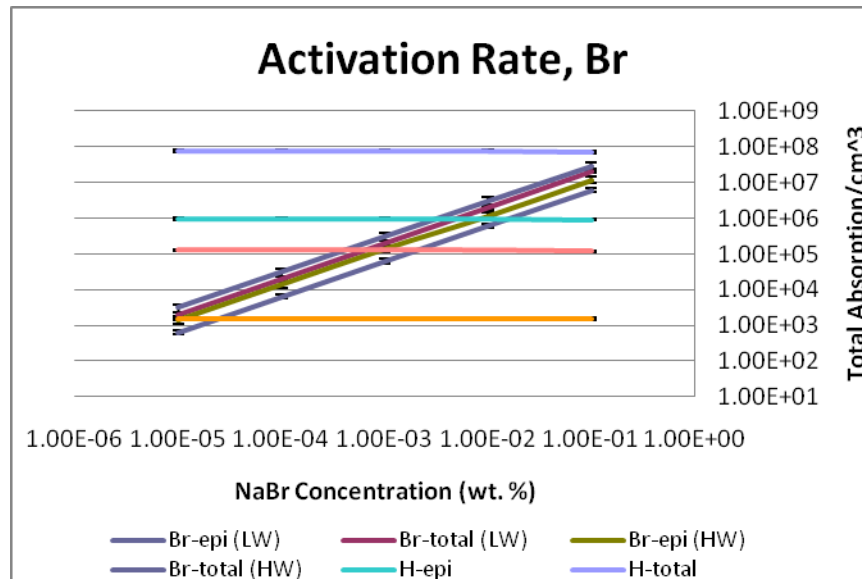


Figure 16, neutron activation rate of Br in light water and heavy water

In addition, within statistical uncertainties there was no difference in the activation rates for the Cl when heavy water was substituted for light water in figure 15; but such result was not repeated for Br. Comparison made in figure 17 revealed a 50%~100% higher activation rate for Br in heavy water solution than in light water. Also note, in both light water and heavy water, epithermal neutron activation rate accounted for about 30%~45% of the total activation rate. All these results are likely due to Br's smaller neutron cross section compared to that of hydrogen and chlorine.

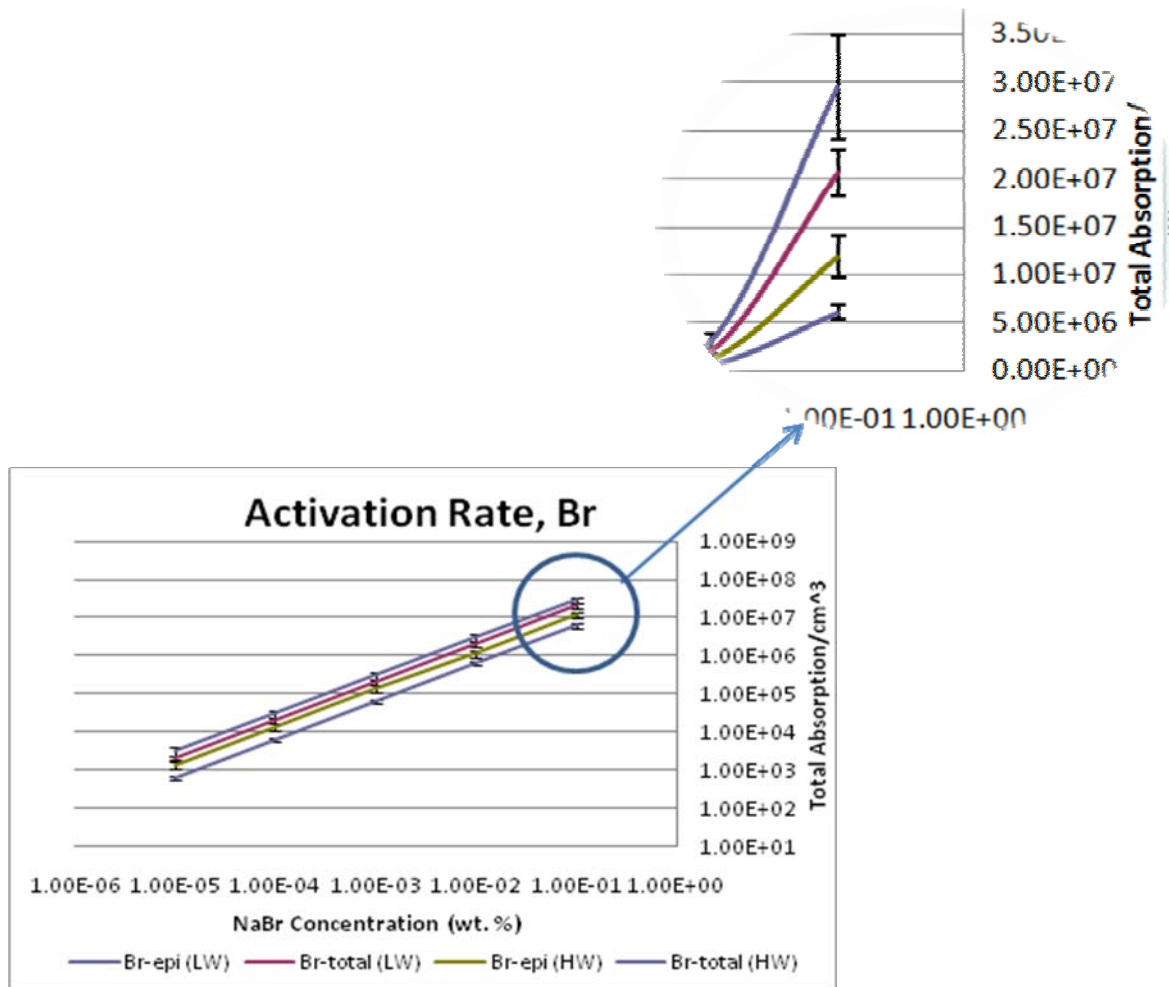


Figure 17, Comparison for neutron activation rate of Br in light water and heavy water

For neutron activation rate of Cl with cadmium shield, figure 18 showed that the thermal activation rate of Cl had no significant difference in light water and heavy water solution; epithermal activation rate, on the other hand, has a 25% higher rate in heavy water than in light water. Note that epithermal neutron activation rate now only was about one order of magnitude lower than thermal neutron activation rate.

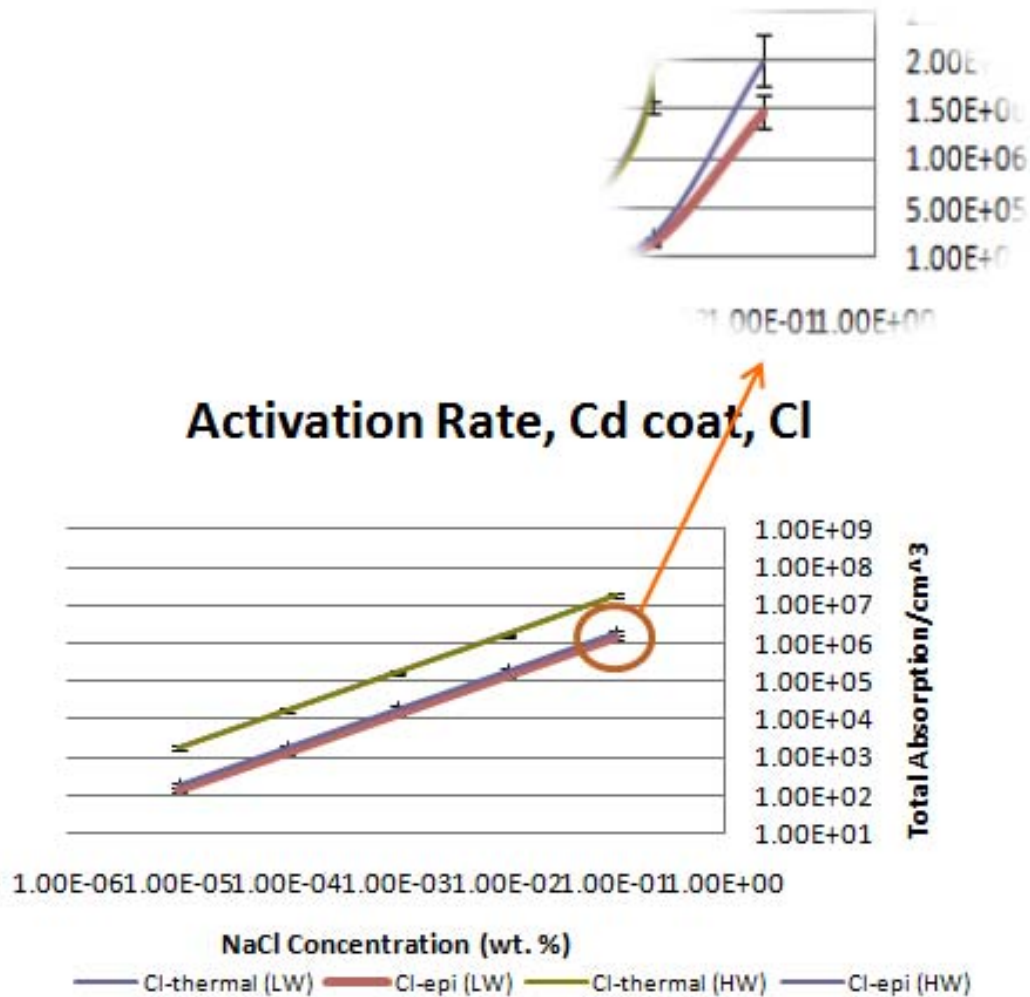


Figure 18, neutron activation rate of Cl with Cd shielding in light water and heavy water

A direct comparison of Cl's neutron activation rate with and without the presence of cadmium shielding was plotted in figure 19 for light water, and figure 20 for heavy water. Note the use of cadmium shielding reduced the epithermal neutron activation rate by 90%, while epithermal neutron activation rate was statistically unchanged.

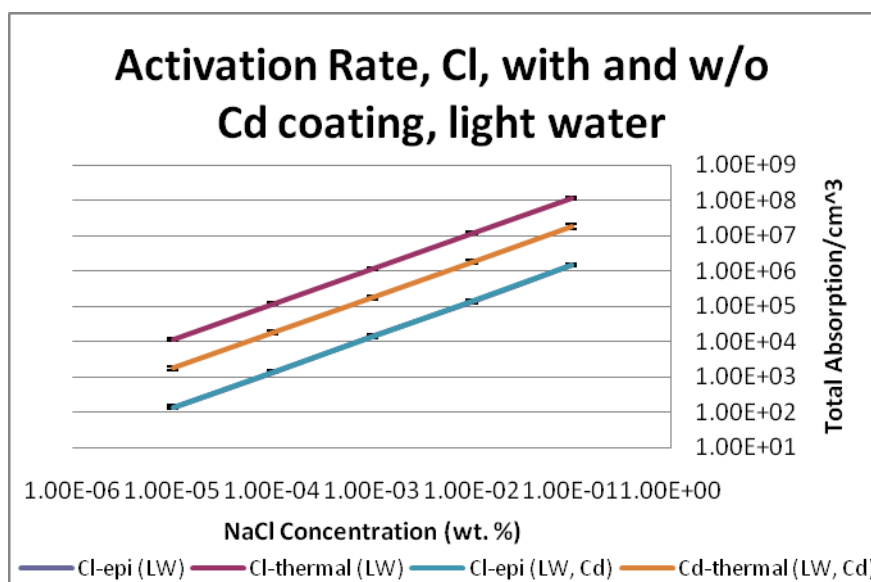


Figure 19, comparison of neutron activation rate of Cl with and without Cd shielding in light water

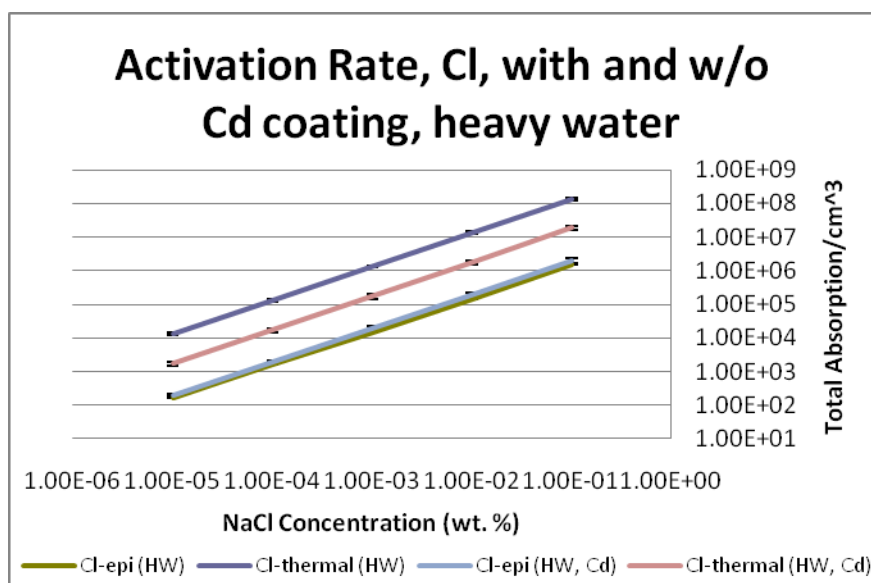


Figure 20, comparison of neutron activation rate of Cl with and without Cd shielding in heavy water

The result in figure 21 for Br with cadmium shielding was more interesting. For both light water and heavy water solution, the thermal neutron activation rates of Br dropped for about 90%; and both were virtually the same. Now, the thermal neutron

activation rate for Br in both light water and heavy water was about 15~20% of epithermal neutron activation rate. In addition, the epithermal neutron activation rate for Br in light water solution went up 40% with no statistically significant change in the heavy water solution; however, the heavy water solution still had a 35% higher Br epithermal neutron activation rate than did the light water solution.

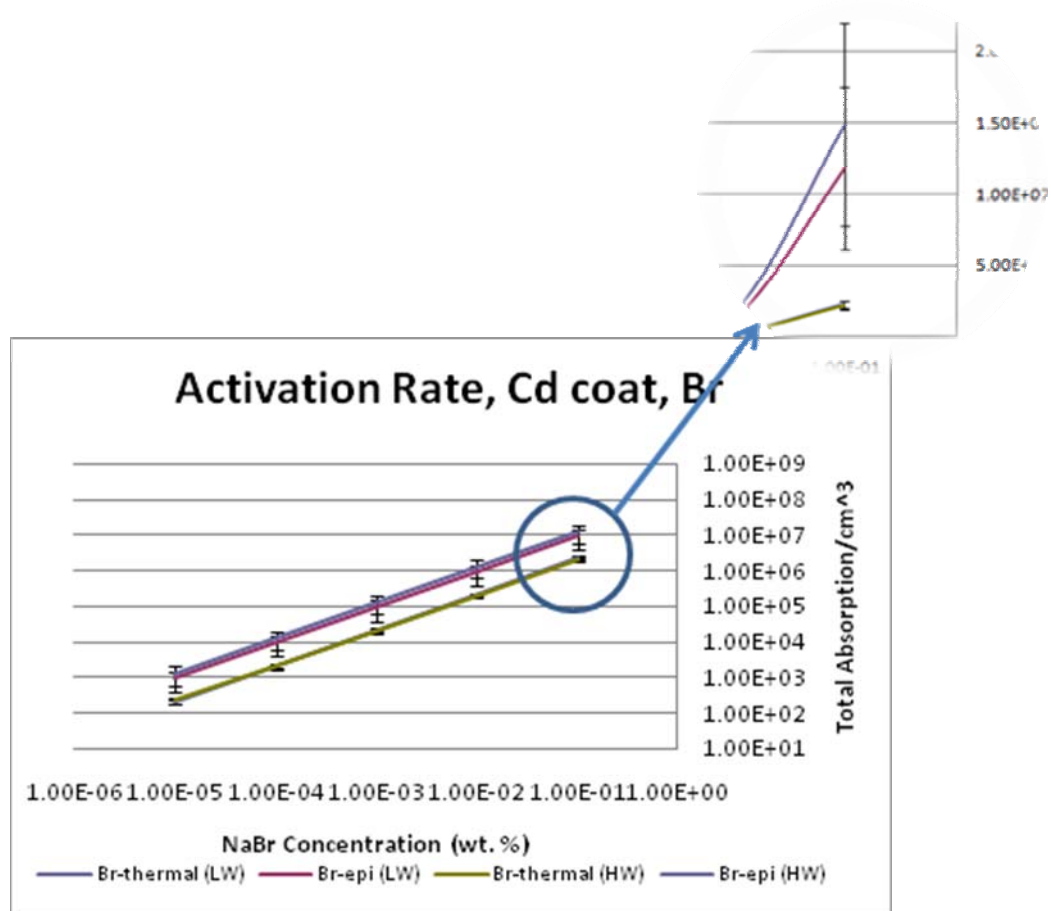


Figure 21, neutron activation rate of Br with Cd shielding in light water and heavy water

It is possible that the higher cross section of the light water effectively 'shields' the Cl and Br by absorbing neutrons in light water. It is also possible that the hydrogen ions downscattered higher energy neutrons in light water, therefore leading to a greater thermalization of epithermal neutrons that did pass through the Cd; these thermalized

neutrons were subsequently more likely to be absorbed by the surrounding Cd. It is more likely that hydrogen within the sample vials competed against Br with thermal & epithermal neutron for activation. In the heavy water solution, this effect was not observed and the Br activation rate was considerably higher.

Neutron Activation Analysis

Due to the tight reactor time schedule, the first batch of sample of NaCl was tested through thermal and epithermal neutron analysis on May 5th. The detailed experimental data analysis will be done in the next stage of this study.

Conclusion

In the absence of cadmium, the simulation did not find consistent discrepancy of neutron activation rate between light water and heavy water solution from the hydrogen shielding effect. In the presence of cadmium, a higher activation rate (~25%) in the heavy water solution compared to light water solution was observed, which was likely the same discrepancy encountered by Dr. Landsberger.

This phenomenon is likely due to the thermalization and absorption of epithermal neutrons of hydrogen from water solution. The next stage of the study will simulate the neutron activation rate of selected isotopes of Cl-35, Br-81 & Br-79 separately in the sample (which follows the natural abundance) to compare more directly with experimental results. In addition, more experimental neutron activation data would be collected to repeat and verify this simulation observation.

References

- [1] X-5 Monte Carlo Team, *MCNP-A General Monte Carlo N-Particle Transport code, V5, Vol II: User's Guide*, Los Alamos, 2005 Rev.
- [2] R. Sher, *Handbook on Nuclear Activation Cross-Sections Technical Report Series No. 156*, International Atomic Energy Agency, Vienna, 1970, pp233-285. International Atomic Energy Agency, Vienna, 1974, pp233-285.
- [3] J. Moteff *Neutron Fluence measurements Technical Report Series No. 107*, International Atomic Energy Agency, Vienna, 1970, pp233-285.
- [4] T.I. Taylor, R.H. Anderson, W.W. Havens Jr., *Science*, 114 (1951) 391.
- [5] K.H. Beckurts, K. Wirtz, *Neutron Physics, Part III*, Springer, Berlin, Germany, 1964, pp233-285.
- [6] W.H. El-Abbadly, Z.H. El-Tananhy, A. A. El-Hagg., *Czech. J. Phys.*, 49 (1999) 1079.
- [7] L. Zikovsky, K. Soliman, *J. Radioanal. Nucl. Chem.*, 240 (1999) 681.
- [8] C. Chilian, J. St-Pierrer, G. Kennedy, *Nucl. Instr. and Meth. A* 564 (2006) 629.
- [9] E. martinho, I.F. Goncalves, J. Salgado, *Appl. Radiat. Isot.* 58 (2003) 371.
- [10] J.D. Braisted Design and Characterization of an Irradiation Facility for Radiation Effects Testing of Electronics with Real-Time Monitoring. Thesis, University of Texas at Austin, 2008.
- [11] P.P.Wilson, P. Snouffer, E.A. Schneider, J. Peteson, *Demonstrating High Fidelity Coupled Neutronic and Thermal Analysis of ART Experiments Report*, Advanced Test Reactor national Scientific User Facility, Idaho National Laboratory, Idaho Fall, 2009, pp48.
- [12] B. Diacon, *Neutron activation Analysis*, Engineering Physics, McMaster University
- [13] G.F. Knoll, *Raiation Detection and measurement, 2nd Ed.*, John Wiley & Sons, Canada, Ltd., 1989.
- [14] M.D. Glascock, *Tables for Neutron Activation Analysis, 4th Ed.*, The University of Missouri, 1996.
- [15] C.E. Crouthamel, *Applied Gamma-Ray Spectrosocopy, 2nd Ed.*, Pergamon Press, Oxford, 1970, pp740-747.

Appendix

Tables

Table A Atomic Number Density

Table B Activation Rate with and without cadmium

MCNPX Simulation Code

Short code with surface source

Long code with TRIGA deck

Table A, Number Density Calculation for Select Elements

	1.00E-05	0.01%	0.10%	1%	10%
Light Water Solution					
NaCl	1.00E-05	1.00E-04	1.00E-03	1.00E-02	1.00E-01
Density (g/cm ³)	1	1	1	1.005	1.07
Nd (water)	3.34147E+22	3.34147E+22	3.34147E+22	3.3246E+22	3.21784E+22
Nd (O)	3.34147E+22	3.34147E+22	3.34147E+22	3.3246E+22	3.21784E+22
Nd (H)	6.68295E+22	6.68295E+22	6.68295E+22	6.6492E+22	6.43568E+22
Nd (Na, Cl)	1.03012E+17	1.03012E+18	1.03012E+19	1.03527E+20	1.10222E+21
scale factor:	4.36E+14				
Nd (H)	2.91E+13	2.91E+13	2.91E+13	2.90E+13	2.81E+13
Nd (Na, Cl)	4.49E+07	4.49E+08	4.49E+09	4.51E+10	4.81E+11

Heavy Water Solution					
NaCl	1.00E-05	1.00E-04	1.00E-03	1.00E-02	1.00E-01
Density (g/cm ³)	1.1056	1.1056	1.1056	1.1056	1.17
Nd (heavy water)	3.32121E+22	3.32121E+22	3.32121E+22	3.288E+22	3.1632E+22
Nd (O)	3.32121E+22	3.32121E+22	3.32121E+22	3.288E+22	3.1632E+22
Nd (D)	6.64243E+22	6.64243E+22	6.64243E+22	6.576E+22	6.32641E+22
Nd (Na, Cl)	1.1389E+17	1.1389E+18	1.1389E+19	1.1389E+20	1.20524E+21
scale factor:	4.36E+14				
Nd (D)	2.90E+13	2.90E+13	2.90E+13	2.87E+13	2.76E+13
Nd (Na, Cl)	4.97E+07	4.97E+08	4.97E+09	4.97E+10	5.25E+11

	1.00E-05	0.01%	0.10%	1%	10%
Light Water Solution					
NaBr	1.00E-05	1.00E-04	1.00E-03	1.00E-02	1.00E-01
Density (g/cm ³)	1	1	1	1.005	1.07
Nd (water)	3.34147E+22	3.34147E+22	3.34147E+22	3.3246E+22	3.21784E+22
Nd (O)	3.34147E+22	3.34147E+22	3.34147E+22	3.3246E+22	3.21784E+22
Nd (H)	6.68295E+22	6.68295E+22	6.68295E+22	6.6492E+22	6.43568E+22
Nd (Na, Br)	5.85068E+16	5.85068E+17	5.85068E+18	5.87993E+19	6.26023E+20
scale factor:	4.36E+14				
Nd (H)	2.91E+13	2.91E+13	2.91E+13	2.90E+13	2.81E+13
Nd (Na, Br)	2.55E+07	2.55E+08	2.55E+09	2.56E+10	2.73E+11

Heavy Water Solution					
NaBr	1.00E-05	1.00E-04	1.00E-03	1.00E-02	1.00E-01
Density (g/cm ³)	1.1056	1.1056	1.1056	1.1056	1.17
Nd (heavy water)	3.32121E+22	3.32121E+22	3.32121E+22	3.288E+22	3.1632E+22
Nd (O)	3.32121E+22	3.32121E+22	3.32121E+22	3.288E+22	3.1632E+22
Nd (D)	6.64243E+22	6.64243E+22	6.64243E+22	6.576E+22	6.32641E+22
Nd (Na, Br)	6.46851E+16	6.46851E+17	6.46851E+18	6.46851E+19	6.8453E+20
scale factor:	4.36E+14				
Nd (D)	2.90E+13	2.90E+13	2.90E+13	2.87E+13	2.76E+13
Nd (Na, Br)	2.82E+07	2.82E+08	2.82E+09	2.82E+10	2.98E+11

Table B, Activation Rate for Selected Elements

With Cd Coating

Br

L.W. concen.	activation rate									activation probability per atom								
	thermal	error %	error	epi	error %	error	total	error %	error	thermal	error %	error	epi	error %	error	total	error %	error
1.00E-05	2.11E+02	1.18E-01	2.50E+01	9.16E+02	4.74E-01	4.34E+02	1.13E+03	1.18E-01	1.33E+02	3.61E-15	1.18E-01	4.27E-16	1.57E-14	4.74E-01	7.42E-15	1.93E-14	1.18E-01	2.27E-15
0.01%	2.11E+03	1.18E-01	2.50E+02	9.16E+03	4.74E-01	4.34E+03	1.13E+04	1.18E-01	1.33E+03	3.61E-15	1.18E-01	4.27E-16	1.57E-14	4.74E-01	7.42E-15	1.93E-14	1.18E-01	2.27E-15
0.10%	2.11E+04	1.18E-01	2.50E+03	9.16E+04	4.74E-01	4.34E+04	1.13E+05	1.18E-01	1.33E+04	3.62E-15	1.18E-01	4.27E-16	1.57E-14	4.74E-01	7.42E-15	1.93E-14	1.18E-01	2.27E-15
1%	2.12E+05	1.18E-01	2.51E+04	9.17E+05	4.74E-01	4.35E+05	1.13E+06	1.18E-01	1.33E+05	3.61E-15	1.18E-01	4.27E-16	1.56E-14	4.74E-01	7.40E-15	1.92E-14	1.18E-01	2.27E-15
10%	2.26E+06	1.18E-01	2.67E+05	9.53E+06	4.81E-01	4.59E+06	1.18E+07	1.18E-01	1.39E+06	3.61E-15	1.18E-01	4.26E-16	1.52E-14	4.81E-01	7.33E-15	1.88E-14	1.18E-01	2.23E-15
H																		
1.00E-05	1.15E+07	1.18E-01	1.35E+06	1.01E+06	1.10E-01	1.11E+05	1.25E+07	1.18E-01	1.47E+06	1.72E-16	1.18E-01	2.03E-17	1.51E-17	1.10E-01	1.66E-18	1.87E-16	1.18E-01	2.21E-17
0.01%	1.15E+07	1.18E-01	1.35E+06	1.01E+06	1.10E-01	1.11E+05	1.25E+07	1.18E-01	1.47E+06	1.72E-16	1.18E-01	2.03E-17	1.51E-17	1.10E-01	1.66E-18	1.87E-16	1.18E-01	2.21E-17
0.10%	1.15E+07	1.18E-01	1.35E+06	1.01E+06	1.10E-01	1.11E+05	1.25E+07	1.18E-01	1.47E+06	1.72E-16	1.18E-01	2.03E-17	1.51E-17	1.10E-01	1.66E-18	1.87E-16	1.18E-01	2.21E-17
1%	1.14E+07	1.18E-01	1.35E+06	1.01E+06	1.10E-01	1.11E+05	1.24E+07	1.18E-01	1.47E+06	1.72E-16	1.18E-01	2.03E-17	1.51E-17	1.10E-01	1.66E-18	1.87E-16	1.18E-01	2.21E-17
10%	1.10E+07	1.18E-01	1.31E+06	9.78E+05	1.10E-01	1.08E+05	1.20E+07	1.18E-01	1.42E+06	1.72E-16	1.18E-01	2.03E-17	1.52E-17	1.10E-01	1.67E-18	1.87E-16	1.18E-01	2.21E-17

H. W.	activation rate									activation probability per atom								
	thermal	error %	error	epi	error %	error	total	error %	error	thermal	error %	error	epi	error %	error	total	error %	error
1.00E-05	2.20E+02	1.45E-01	3.18E+01	1.30E+03	4.63E-01	6.02E+02	1.52E+03	1.45E-01	2.20E+02	3.40E-15	1.45E-01	4.92E-16	2.01E-14	4.63E-01	9.31E-15	2.35E-14	1.45E-01	3.40E-15
0.01%	2.02E+03	1.45E-01	2.92E+02	1.32E+04	4.63E-01	6.11E+03	1.52E+04	1.45E-01	2.20E+03	3.12E-15	1.45E-01	4.52E-16	2.04E-14	4.63E-01	9.44E-15	2.35E-14	1.45E-01	3.40E-15
0.10%	2.02E+04	1.45E-01	2.92E+03	1.32E+05	4.63E-01	6.11E+04	1.52E+05	1.45E-01	2.20E+04	3.12E-15	1.45E-01	4.52E-16	2.04E-14	4.63E-01	9.44E-15	2.35E-14	1.45E-01	3.40E-15
1%	2.02E+05	1.45E-01	2.92E+04	1.31E+06	4.66E-01	6.09E+05	1.51E+06	1.45E-01	2.18E+05	3.11E-15	1.45E-01	4.50E-16	2.01E-14	4.66E-01	9.37E-15	2.32E-14	1.45E-01	3.36E-15
10%	2.17E+06	1.44E-01	3.11E+05	1.27E+07	4.80E-01	6.08E+06	1.48E+07	1.44E-01	2.13E+06	3.16E-15	1.44E-01	4.55E-16	1.85E-14	4.80E-01	8.88E-15	2.17E-14	1.44E-01	3.12E-15
D																		
1.00E-05	1.60E+04	1.45E-01	2.31E+03	1.10E+03	1.29E-01	1.41E+02	1.70E+04	1.45E-01	2.47E+03	2.40E-19	1.45E-01	3.48E-20	1.65E-20	1.29E-01	2.12E-21	2.57E-19	1.45E-01	3.71E-20
0.01%	1.51E+04	1.45E-01	2.18E+03	2.00E+03	1.29E-01	2.57E+02	1.70E+04	1.45E-01	2.47E+03	2.27E-19	1.45E-01	3.28E-20	3.00E-20	1.29E-01	3.87E-21	2.57E-19	1.45E-01	3.71E-20
0.10%	1.51E+04	1.45E-01	2.18E+03	1.99E+03	1.29E-01	2.57E+02	1.70E+04	1.45E-01	2.47E+03	2.27E-19	1.45E-01	3.28E-20	3.00E-20	1.29E-01	3.87E-21	2.57E-19	1.45E-01	3.71E-20
1%	1.49E+04	1.45E-01	2.16E+03	1.97E+03	1.29E-01	2.54E+02	1.69E+04	1.45E-01	2.44E+03	2.26E-19	1.45E-01	3.28E-20	3.00E-20	1.29E-01	3.86E-21	2.56E-19	1.45E-01	3.71E-20
10%	1.45E+04	1.44E-01	2.09E+03	1.89E+03	1.28E-01	2.43E+02	1.64E+04	1.44E-01	2.36E+03	2.29E-19	1.44E-01	3.30E-20	2.99E-20	1.28E-01	3.83E-21	2.59E-19	1.44E-01	3.73E-20

Cl

L.W.	activation rate									activation probability per atom								
	thermal	error %	error	epi	error %	error	total	error %	error	thermal	error %	error	epi	error %	error	total	error %	error
1.00E-05	1.79E+03	1.18E-01	2.12E+02	1.42E+02	1.40E-01	1.98E+01	1.93E+03	1.40E-01	2.70E+02	1.74E-14	1.18E-01	2.06E-15	1.38E-15	1.40E-01	1.92E-16	1.88E-14	1.40E-01	2.62E-15
0.01%	1.79E+04	1.18E-01	2.12E+03	1.42E+03	1.11E-01	1.57E+02	1.93E+04	1.11E-01	2.14E+03	1.74E-14	1.18E-01	2.06E-15	1.38E-15	1.11E-01	1.53E-16	1.88E-14	1.11E-01	2.08E-15
0.10%	1.79E+05	1.18E-01	2.12E+04	1.42E+04	1.11E-01	1.57E+03	1.93E+05	1.11E-01	2.14E+04	1.74E-14	1.18E-01	2.06E-15	1.37E-15	1.11E-01	1.52E-16	1.88E-14	1.11E-01	2.08E-15
1%	1.80E+06	1.18E-01	2.13E+05	1.43E+05	1.11E-01	1.58E+04	1.94E+06	1.11E-01	2.15E+05	1.74E-14	1.18E-01	2.06E-15	1.38E-15	1.11E-01	1.53E-16	1.88E-14	1.11E-01	2.08E-15
10%	1.86E+07	1.16E-01	2.15E+06	1.48E+06	1.08E-01	1.60E+05	2.01E+07	1.08E-01	2.17E+06	1.69E-14	1.16E-01	1.95E-15	1.34E-15	1.08E-01	1.46E-16	1.82E-14	1.08E-01	1.98E-15
H																		
1.00E-05	1.15E+07	1.18E-01	1.35E+06	1.01E+06	1.10E-01	1.11E+05	1.25E+07	1.10E-01	1.37E+06	1.72E-16	1.18E-01	2.03E-17	1.51E-17	1.10E-01	1.66E-18	1.87E-16	1.10E-01	2.05E-17
0.01%	1.15E+07	1.18E-01	1.35E+06	1.01E+06	1.10E-01	1.11E+05	1.25E+07	1.10E-01	1.37E+06	1.72E-16	1.18E-01	2.03E-17	1.51E-17	1.10E-01	1.66E-18	1.87E-16	1.10E-01	2.05E-17
0.10%	1.15E+07	1.18E-01	1.35E+06	1.01E+06	1.10E-01	1.11E+05	1.25E+07	1.10E-01	1.37E+06	1.72E-16	1.18E-01	2.03E-17	1.51E-17	1.10E-01	1.66E-18	1.87E-16	1.10E-01	2.05E-17
1%	1.14E+07	1.18E-01	1.35E+06	1.01E+06	1.10E-01	1.11E+05	1.24E+07	1.10E-01	1.37E+06	1.72E-16	1.18E-01	2.03E-17	1.51E-17	1.10E-01	1.66E-18	1.87E-16	1.10E-01	2.06E-17
10%	1.07E+07	1.16E-01	1.24E+06	9.53E+05	1.08E-01	1.02E+05	1.17E+07	1.08E-01	1.25E+06	1.67E-16	1.16E-01	1.93E-17	1.48E-17	1.08E-01	1.59E-18	1.82E-16	1.08E-01	1.95E-17

activation rate

activation probability per atom

H. W.	thermal Cl	error %	error	epi	error %	error	total	error %	error	thermal	error %	error	epi	error %	error	total	error %	error
1.00E-05	1.72E+03	1.45E-01	2.49E+02	1.94E+02	1.31E-01	2.55E+01	1.91E+03	1.31E-01	2.50E+02	1.51E-14	1.45E-01	2.18E-15	1.70E-15	1.31E-01	2.23E-16	1.68E-14	1.31E-01	2.20E-15
0.01%	1.72E+04	1.45E-01	2.49E+03	1.94E+03	1.31E-01	2.55E+02	1.91E+04	1.31E-01	2.50E+03	1.51E-14	1.45E-01	2.18E-15	1.70E-15	1.31E-01	2.23E-16	1.68E-14	1.31E-01	2.20E-15
0.10%	1.72E+05	1.45E-01	2.49E+04	1.94E+04	1.31E-01	2.55E+03	1.91E+05	1.31E-01	2.50E+04	1.51E-14	1.45E-01	2.18E-15	1.70E-15	1.31E-01	2.23E-16	1.68E-14	1.31E-01	2.20E-15
1%	1.71E+06	1.45E-01	2.49E+05	1.93E+05	1.31E-01	2.54E+04	1.91E+06	1.31E-01	2.50E+05	1.51E-14	1.45E-01	2.18E-15	1.70E-15	1.31E-01	2.23E-16	1.68E-14	1.31E-01	2.20E-15
10%	1.86E+07	1.48E-01	2.75E+06	2.00E+06	1.35E-01	2.70E+05	2.06E+07	1.35E-01	2.77E+06	1.54E-14	1.48E-01	2.28E-15	1.66E-15	1.35E-01	2.23E-16	1.70E-14	1.35E-01	2.29E-15
D																		
1.00E-05	1.51E+04	1.45E-01	2.18E+03	2.00E+03	1.29E-01	2.57E+02	1.70E+04	1.29E-01	2.19E+03	2.27E-19	1.45E-01	3.28E-20	3.01E-20	1.29E-01	3.87E-21	2.57E-19	1.29E-01	3.30E-20
0.01%	1.51E+04	1.45E-01	2.18E+03	2.00E+03	1.29E-01	2.57E+02	1.70E+04	1.29E-01	2.19E+03	2.27E-19	1.45E-01	3.28E-20	3.01E-20	1.29E-01	3.87E-21	2.57E-19	1.29E-01	3.30E-20
0.10%	1.49E+04	1.45E-01	2.16E+03	2.15E+03	1.29E-01	2.77E+02	1.70E+04	1.29E-01	2.19E+03	2.24E-19	1.45E-01	3.25E-20	3.24E-20	1.29E-01	4.17E-21	2.57E-19	1.29E-01	3.30E-20
1%	1.49E+04	1.45E-01	2.15E+03	1.97E+03	1.29E-01	2.54E+02	1.69E+04	1.29E-01	2.17E+03	2.26E-19	1.45E-01	3.27E-20	2.99E-20	1.29E-01	3.85E-21	2.56E-19	1.29E-01	3.30E-20
10%	1.47E+04	1.48E-01	2.17E+03	1.86E+03	1.32E-01	2.45E+02	1.65E+04	1.32E-01	2.18E+03	2.32E-19	1.48E-01	3.43E-20	2.93E-20	1.32E-01	3.87E-21	2.61E-19	1.32E-01	3.45E-20

Without Cd Coating Br

L.W.	activation rate									activation probability per atom								
	thermal	error %	error	epi	error %	error	total	error %	error	thermal	error %	error	epi	error %	error	total	error %	error
Br																		
1.00E-05	1.39E+03	7.13E-02	9.92E+01	6.37E+02	1.33E-01	8.46E+01	2.03E+03	1.33E-01	2.69E+02	2.38E-14	7.13E-02	1.70E-15	1.09E-14	1.33E-01	1.45E-15	3.47E-14	1.33E-01	4.60E-15
0.01%	1.39E+04	7.13E-02	9.92E+02	6.37E+03	1.33E-01	8.46E+02	2.03E+04	1.33E-01	2.69E+03	2.38E-14	7.13E-02	1.70E-15	1.09E-14	1.33E-01	1.45E-15	3.47E-14	1.33E-01	4.60E-15
0.10%	1.39E+05	7.13E-02	9.90E+03	6.37E+04	1.33E-01	8.45E+03	2.03E+05	1.33E-01	2.69E+04	2.37E-14	7.13E-02	1.69E-15	1.09E-14	1.33E-01	1.44E-15	3.46E-14	1.33E-01	4.60E-15
1%	1.39E+06	7.11E-02	9.85E+04	6.34E+05	1.31E-01	8.27E+04	2.02E+06	1.31E-01	2.64E+05	2.36E-14	7.11E-02	1.68E-15	1.08E-14	1.31E-01	1.41E-15	3.44E-14	1.31E-01	4.48E-15
10%	1.45E+07	6.98E-02	1.01E+06	6.08E+06	1.16E-01	7.05E+05	2.05E+07	1.16E-01	2.38E+06	2.31E-14	6.98E-02	1.61E-15	9.71E-15	1.16E-01	1.13E-15	3.28E-14	1.16E-01	3.80E-15
H																		
1.00E-05	7.54E+07	7.13E-02	5.37E+06	9.52E+05	7.05E-02	6.71E+04	7.64E+07	7.05E-02	5.39E+06	1.13E-15	7.13E-02	8.04E-17	1.43E-17	7.05E-02	1.00E-18	1.14E-15	7.05E-02	8.06E-17
0.01%	7.55E+07	7.13E-02	5.38E+06	9.52E+05	7.05E-02	6.71E+04	7.64E+07	7.05E-02	5.39E+06	1.13E-15	7.13E-02	8.06E-17	1.43E-17	7.05E-02	1.00E-18	1.14E-15	7.05E-02	8.06E-17
0.10%	7.54E+07	7.13E-02	5.38E+06	9.52E+05	7.05E-02	6.71E+04	7.65E+07	7.05E-02	5.39E+06	1.13E-15	7.13E-02	8.05E-17	1.43E-17	7.05E-02	1.00E-18	1.15E-15	7.05E-02	8.07E-17
1%	7.47E+07	7.11E-02	5.31E+06	9.50E+05	7.03E-02	6.68E+04	7.56E+07	7.03E-02	5.31E+06	1.12E-15	7.11E-02	7.98E-17	1.43E-17	7.03E-02	1.00E-18	1.14E-15	7.03E-02	7.99E-17
10%	7.08E+07	6.99E-02	4.95E+06	9.13E+05	6.90E-02	6.30E+04	7.17E+07	6.90E-02	4.95E+06	1.10E-15	6.99E-02	7.69E-17	1.42E-17	6.90E-02	9.80E-19	1.12E-15	6.90E-02	7.69E-17
D																		
1.00E-05	1.26E+05	5.88E-02	7.43E+03	1.53E+03	5.81E-02	8.89E+01	1.28E+05	5.81E-02	7.43E+03	1.90E-18	5.88E-02	1.12E-19	2.30E-20	5.81E-02	1.34E-21	1.93E-18	5.81E-02	1.12E-19
0.01%	1.26E+05	5.88E-02	7.43E+03	1.53E+03	5.81E-02	8.89E+01	1.28E+05	5.81E-02	7.43E+03	1.90E-18	5.88E-02	1.12E-19	2.30E-20	5.81E-02	1.34E-21	1.93E-18	5.81E-02	1.12E-19
0.10%	1.27E+05	6.01E-02	7.66E+03	1.50E+03	5.95E-02	8.93E+01	1.29E+05	5.95E-02	7.67E+03	1.92E-18	6.01E-02	1.15E-19	2.26E-20	5.95E-02	1.34E-21	1.94E-18	5.95E-02	1.16E-19
1%	1.25E+05	5.87E-02	7.33E+03	1.50E+03	5.80E-02	8.70E+01	1.26E+05	5.80E-02	7.33E+03	1.90E-18	5.87E-02	1.11E-19	2.28E-20	5.80E-02	1.32E-21	1.92E-18	5.80E-02	1.11E-19
10%	1.18E+05	5.83E-02	6.90E+03	1.51E+03	5.76E-02	8.72E+01	1.20E+05	5.76E-02	6.90E+03	1.87E-18	5.83E-02	1.09E-19	2.39E-20	5.76E-02	1.38E-21	1.89E-18	5.76E-02	1.09E-19
H. W.																		
	activation rate									activation probability per atom								
	thermal	error %	error	epi	error %	error	total	error %	error	thermal	error %	error	epi	error %	error	total	error %	error
Br																		
1.00E-05	1.70E+03	5.88E-02	9.97E+01	1.40E+03	2.30E-01	3.23E+02	3.10E+03	2.30E-01	7.14E+02	2.62E-14	5.88E-02	1.54E-15	2.17E-14	2.30E-01	5.00E-15	4.79E-14	2.30E-01	1.10E-14
0.01%	1.70E+04	5.88E-02	9.97E+02	1.41E+04	2.30E-01	3.24E+03	3.10E+04	2.30E-01	7.14E+03	2.62E-14	5.88E-02	1.54E-15	2.18E-14	2.30E-01	5.01E-15	4.80E-14	2.30E-01	1.10E-14
0.10%	1.71E+05	6.01E-02	1.03E+04	1.41E+05	2.29E-01	3.23E+04	3.12E+05	2.29E-01	7.15E+04	2.64E-14	6.01E-02	1.59E-15	2.18E-14	2.29E-01	4.99E-15	4.82E-14	2.29E-01	1.11E-14
1%	1.93E+06	5.87E-02	1.13E+05	1.17E+06	2.32E-01	2.71E+05	3.10E+06	2.32E-01	7.18E+05	2.97E-14	5.87E-02	1.74E-15	1.80E-14	2.32E-01	4.17E-15	4.77E-14	2.32E-01	1.11E-14
10%	1.76E+07	5.83E-02	1.03E+06	1.19E+07	1.84E-01	2.20E+06	2.96E+07	1.84E-01	5.45E+06	2.57E-14	5.83E-02	1.50E-15	1.74E-14	1.84E-01	3.21E-15	4.32E-14	1.84E-01	7.96E-15

Cl

activation rate

activation probability per atom

L.W.	thermal	error %	error	epi	error %	error	total	error %	error	thermal	error %	error	epi	error %	error	total	error %	error
	Cl																	
1.00E-05	1.18E+04	7.15E-02	8.44E+02	1.41E+02	7.08E-02	1.00E+01	1.19E+04	7.08E-02	8.45E+02	1.15E-13	7.15E-02	8.19E-15	1.37E-15	7.08E-02	9.71E-17	1.16E-13	7.08E-02	8.21E-15
0.01%	1.18E+05	7.15E-02	8.43E+03	1.36E+03	7.08E-02	9.60E+01	1.19E+05	7.08E-02	8.44E+03	1.14E-13	7.15E-02	8.18E-15	1.32E-15	7.08E-02	9.32E-17	1.16E-13	7.08E-02	8.19E-15
0.10%	1.18E+06	7.15E-02	8.43E+04	1.44E+04	7.08E-02	1.02E+03	1.19E+06	7.08E-02	8.45E+04	1.14E-13	7.15E-02	8.18E-15	1.39E-15	7.08E-02	9.86E-17	1.16E-13	7.08E-02	8.20E-15
1%	1.18E+07	7.17E-02	8.46E+05	1.34E+05	7.10E-02	9.51E+03	1.19E+07	7.10E-02	8.47E+05	1.13E-13	7.17E-02	8.13E-15	1.29E-15	7.10E-02	9.14E-17	1.15E-13	7.10E-02	8.14E-15
10%	1.17E+08	7.10E-02	8.30E+06	1.44E+06	7.02E-02	1.01E+05	1.18E+08	7.02E-02	8.30E+06	1.06E-13	7.10E-02	7.54E-15	1.31E-15	7.02E-02	9.19E-17	1.08E-13	7.02E-02	7.55E-15
	H																	
1.00E-05	7.55E+07	7.13E-02	5.38E+06	9.40E+05	7.05E-02	6.63E+04	7.64E+07	7.05E-02	5.39E+06	1.13E-15	7.13E-02	8.05E-17	1.41E-17	7.05E-02	9.92E-19	1.14E-15	7.05E-02	8.06E-17
0.01%	7.54E+07	7.13E-02	5.37E+06	9.30E+05	7.05E-02	6.56E+04	7.63E+07	7.05E-02	5.38E+06	1.13E-15	7.13E-02	8.04E-17	1.39E-17	7.05E-02	9.82E-19	1.14E-15	7.05E-02	8.05E-17
0.10%	7.54E+07	7.13E-02	5.37E+06	1.02E+06	7.05E-02	7.16E+04	7.64E+07	7.05E-02	5.39E+06	1.13E-15	7.13E-02	8.05E-17	1.52E-17	7.05E-02	1.07E-18	1.14E-15	7.05E-02	8.06E-17
1%	7.49E+07	7.15E-02	5.35E+06	9.40E+05	7.07E-02	6.65E+04	7.58E+07	7.07E-02	5.36E+06	1.13E-15	7.15E-02	8.05E-17	1.41E-17	7.07E-02	1.00E-18	1.14E-15	7.07E-02	8.06E-17
10%	6.74E+07	7.08E-02	4.77E+06	8.60E+05	7.00E-02	6.02E+04	6.83E+07	7.00E-02	4.78E+06	1.05E-15	7.08E-02	7.41E-17	1.34E-17	7.00E-02	9.35E-19	1.06E-15	7.00E-02	7.43E-17
	activation rate									activation probability per atom								
H. W.	thermal	error %	error	epi	error %	error	total	error %	error	thermal	error %	error	epi	error %	error	total	error %	error
	Cl																	
1.00E-05	1.32E+04	6.96E-02	9.19E+02	1.70E+02	6.89E-02	1.17E+01	1.34E+04	6.89E-02	9.21E+02	1.16E-13	6.96E-02	8.07E-15	1.49E-15	6.89E-02	1.03E-16	1.17E-13	6.89E-02	8.09E-15
0.01%	1.32E+05	6.96E-02	9.19E+03	1.70E+03	6.96E-02	1.18E+02	1.34E+05	6.96E-02	9.31E+03	1.16E-13	6.96E-02	8.07E-15	1.49E-15	6.96E-02	1.04E-16	1.17E-13	6.96E-02	8.17E-15
0.10%	1.34E+06	7.23E-02	9.72E+04	1.50E+04	7.16E-02	1.07E+03	1.36E+06	7.16E-02	9.73E+04	1.18E-13	7.23E-02	8.53E-15	1.32E-15	7.16E-02	9.43E-17	1.19E-13	7.16E-02	8.54E-15
1%	1.34E+07	7.23E-02	9.68E+05	1.48E+05	7.16E-02	1.06E+04	1.35E+07	7.16E-02	9.69E+05	1.18E-13	7.23E-02	8.50E-15	1.30E-15	7.16E-02	9.30E-17	1.19E-13	7.16E-02	8.51E-15
10%	1.33E+08	6.87E-02	9.12E+06	1.58E+06	6.80E-02	1.07E+05	1.34E+08	6.80E-02	9.14E+06	1.10E-13	6.87E-02	7.54E-15	1.31E-15	6.80E-02	8.88E-17	1.11E-13	6.80E-02	7.55E-15
	D																	
1.00E-05	1.16E+05	6.93E-02	8.04E+03	1.54E+03	6.84E-02	1.05E+02	1.18E+05	6.84E-02	8.04E+03	1.75E-18	6.93E-02	1.21E-19	2.32E-20	6.84E-02	1.58E-21	1.77E-18	6.84E-02	1.21E-19
0.01%	1.16E+05	6.93E-02	8.04E+03	1.54E+03	6.84E-02	1.05E+02	1.18E+05	6.84E-02	8.04E+03	1.75E-18	6.93E-02	1.21E-19	2.32E-20	6.84E-02	1.58E-21	1.77E-18	6.84E-02	1.21E-19
0.10%	1.18E+05	7.20E-02	8.49E+03	1.57E+03	7.11E-02	1.12E+02	1.19E+05	7.11E-02	8.49E+03	1.78E-18	7.20E-02	1.28E-19	2.37E-20	7.11E-02	1.69E-21	1.80E-18	7.11E-02	1.28E-19
1%	1.16E+05	7.20E-02	8.37E+03	1.55E+03	7.11E-02	1.10E+02	1.18E+05	7.11E-02	8.37E+03	1.77E-18	7.20E-02	1.27E-19	2.35E-20	7.11E-02	1.67E-21	1.79E-18	7.11E-02	1.27E-19
10%	1.05E+05	6.84E-02	7.18E+03	1.50E+03	6.76E-02	1.01E+02	1.07E+05	6.76E-02	7.20E+03	1.66E-18	6.84E-02	1.13E-19	2.37E-20	6.76E-02	1.60E-21	1.68E-18	6.76E-02	1.14E-19

Short Code with Surface Source

surface source

c -----

c Tube cell for my test (Alex Zhou 2009)

c -----

9001 9924 -1.17 -9001 \$ solution inside container

9002 99 -.93 -9002 +9001 \$ container of polyethylene

9101 9990 -8.65 -9101 +9002 \$ Cd foil

9012 1 -1 -111 +121 -9010 +9101 \$ cell of surface source

c

c -----

c Outside world

c -----

2999 0 +111: -121: +9010

c surface card

c -----

c upper and lower bounds

c -----

111 pz +3.3 \$ Upper cap of surface source

121 PZ -1.7 \$ Lower cap of surface source

c

c -----

c Tube surface for my test (Alex Zhou 2009)

c -----

9001 rcc +19.59102 +11.31062 0.05 0 0 1.5 0.5 \$sample space inside container
9002 rcc +19.59102 +11.31062 0 0 0 1.6 0.55 \$container of polyethylene
9101 rcc +19.59102 +11.31062 -.01 0 0 1.62 0.56 \$Cd foil
9010 c/z +19.59102 +11.31062 1.5 \$ surface source bound

c data card

c -----

c Tube material for my test (Alex Zhou 2009)

c -----

m1 1001 0.66667

8016 0.33333

m99 1001 2

6012 1

MT99 POLY.60t \$ CH2, polyethylene

m9920 1002 -.20000 \$.001% NaBr heavy water solution

8016 -.79999

11023 -2.24E-6

35081 -3.88E-6

35079 -3.88E-6

m9921 1002 -.2000 \$.01% NaBr heavy water solution

8016 -.7999

11023 -2.24E-5

35081 -3.88E-5

35079 -3.88E-5

m9922 1002 -.200 \$.1% NaBr heavy water solution

8016 -.799

11023 -2.24E-4

35081 -3.88E-4
 35079 -3.88E-4
 m9923 1002 -.20 \$ 1% NaBr heavy water solution
 8016 -.79
 11023 -2.24E-3
 35081 -3.88E-3
 35079 -3.88E-3
 m9924 1002 -.2 \$.001% NaBr heavy water solution
 8016 -.7
 11023 -2.24E-2
 35081 -3.88E-2
 35079 -3.88E-2
 m9992 2001 .667 \$ water
 8016 .333
 m9990 48000 1 \$ cd
 MT9992 hwtr.60c
 m9993 11023 1 \$ Na
 m9994 17000 1 \$ Cl
 m9999 35079 .5069 \$ Br
 35081 .4931
 m9995 1001 1 \$ H
 m9996 1002 1 \$ D2 heavey water
 MT9 POLY.60t
 c
 mode n p
 c phys:p 100 0 0 0 1 -102 \$ -102, Analog sampling, models only, multigroup +
 line emission
 imp:n 1 3r 0

```
imp:p 1 3r 0
c energy band: thermal, epithermal, and fast
ssr old -9010 -111 121
E4 1E-6 1e-3 1
F4:n 9001
FM4 (2.98e+11 9999 -2) (2.76e+13 9996 -2)
FC4
print
```

(The long code with TRIGA deck takes 67 pages; to save paper,
I will submit the electronic version of the code upon request)

Long Code with TRIGA Deck

c-----UT TRIGA -Core Model -07/12/2007 -----

c

c -----

c Beginning of Cell Card Specification

c -----

c -----

c Core region

c -----

1099 1 -1.0 -202 +206

-231 +232 -233 +234 -235 +236

-241 +242 -243 +244 -245 +246

+5000 +5001 +5002 +5003 +5004 +5005 +5006 +5007 +5008 +5009

+5010 +5011 +5012 +5013 +5014 +5015 +5016 +5017 +5018 +5019

+5020 +5021 +5022 +5023 +5024 +5025 +5026 +5027 +5028 +5029

+5030 +5031 +5032 +5033 +5034 +5035 +5036 +5037 +5038

+5041 +5042 +5043 +5044 +5045 +5046 +5048 +5049

+5050 +5051 +5052 +5053 +5054 +5055 +5056 +5057 +5058 +5059

+5060 +5061 +5062 +5066 +5067 +5068 +5069

+5070 +5071 +5072 +5075 +5076 +5077 +5078 +5079

+5080 +5081 +5082 +5083 +5084 +5085 +5086 +5087 +5088 +5089

+5090 +5091 +5092 +5095 +5096 +5097 +5098 +5099

+5100 +5102 +5103 +5104 +5105 +5106 +5107 +5108 +5109

+5110 +5112 +5113 +5114 +5117 +5118 +5119

+5120

+1963 +1964 +1965 +1966 \$ Mapping experiment
 +5101
 +1940 \$ 6L
 +5047 +5073 +5074 \$ Elements in 3L
 +2000 +2001 +2002 +2003 +2004 +2005 +2006
 c +5111 +5115
 c +5039 +5040 +5063 +5064 +5065 +5093 +5094 \$ Elements in 6L
 c +961 \$ 3L
 c +5118 \$ PNT
 c
 520 0 -201 +207 -1963 fill=101 (10) \$ Flux mapping water cells
 521 0 -201 +207 -1964 fill=101 (11)
 522 0 -201 +207 -1965 fill=101 (12)
 523 0 -201 +207 -1966 fill=101 (13)
 c
 600 0 -110 +120 -5000 fill=82 (100) \$ A1 Fuel & graphite elements
 601 0 -110 +120 -5001 fill=8 (101) \$ B1 Control rods
 602 0 -110 +120 -5002 fill=8 (102) \$ B2
 603 0 -110 +120 -5003 fill=8 (103) \$ B3
 604 0 -110 +120 -5004 fill=8 (104) \$ B4
 605 0 -110 +120 -5005 fill=8 (105) \$ B5
 606 0 -110 +120 -5006 fill=8 (106) \$ B6
 607 0 -110 +120 -5007 fill=7 (107) \$ C1 -CR(T)
 608 0 -110 +120 -5008 fill=8 (108) \$ C2
 609 0 -110 +120 -5009 fill=8 (109) \$ C3
 610 0 -110 +120 -5010 fill=8 (110) \$ C4
 611 0 -110 +120 -5011 fill=8 (111) \$ C5

612 0 -110 +120 -5012 fill=8 (112) \$ C6
613 0 -110 +120 -5013 fill=9 (113) \$ C7 -CR(R)
614 0 -110 +120 -5014 fill=8 (114) \$ C8
615 0 -110 +120 -5015 fill=8 (115) \$ C9
616 0 -110 +120 -5016 fill=8 (116) \$ C10
617 0 -110 +120 -5017 fill=8 (117) \$ C11
618 0 -110 +120 -5018 fill=8 (118) \$ C12
619 0 -110 +120 -5019 fill=8 (119) \$ D1
620 0 -110 +120 -5020 fill=8 (120) \$ D2
621 0 -110 +120 -5021 fill=8 (121) \$ D3
622 0 -110 +120 -5022 fill=8 (122) \$ D4
623 0 -110 +120 -5023 fill=8 (123) \$ D5
624 0 -110 +120 -5024 fill=9 (124) \$ D6 -CR(S)
625 0 -110 +120 -5025 fill=8 (125) \$ D7
626 0 -110 +120 -5026 fill=8 (126) \$ D8
627 0 -110 +120 -5027 fill=8 (127) \$ D9
628 0 -110 +120 -5028 fill=8 (128) \$ D10
629 0 -110 +120 -5029 fill=8 (129) \$ D11
630 0 -110 +120 -5030 fill=8 (130) \$ D12
631 0 -110 +120 -5031 fill=8 (131) \$ D13
632 0 -110 +120 -5032 fill=9 (132) \$ D14 -CR(S)
633 0 -110 +120 -5033 fill=8 (133) \$ D15
634 0 -110 +120 -5034 fill=8 (134) \$ D16
635 0 -110 +120 -5035 fill=8 (135) \$ D17
636 0 -110 +120 -5036 fill=8 (136) \$ D18
637 0 -110 +120 -5037 fill=8 (137) \$ E1
638 0 -110 +120 -5038 fill=8 (138) \$ E2

c 639 0 -110 +120 -5039 fill=8 (139) \$ E3
c 640 0 -110 +120 -5040 fill=8 (140) \$ E4
641 0 -110 +120 -5041 fill=8 (141) \$ E5
642 0 -110 +120 -5042 fill=8 (142) \$ E6
643 0 -110 +120 -5043 fill=8 (143) \$ E7
644 0 -110 +120 -5044 fill=8 (144) \$ E8
645 0 -110 +120 -5045 fill=8 (145) \$ E9
646 0 -110 +120 -5046 fill=8 (146) \$ E10
647 0 -110 +120 -5047 fill=8 (147) \$ E11
648 0 -110 +120 -5048 fill=8 (148) \$ E12
649 0 -110 +120 -5049 fill=8 (149) \$ E13
650 0 -110 +120 -5050 fill=8 (150) \$ E14
651 0 -110 +120 -5051 fill=8 (151) \$ E15
652 0 -110 +120 -5052 fill=8 (152) \$ E16
653 0 -110 +120 -5053 fill=8 (153) \$ E17
654 0 -110 +120 -5054 fill=8 (154) \$ E18
655 0 -110 +120 -5055 fill=8 (155) \$ E19
656 0 -110 +120 -5056 fill=8 (156) \$ E20
657 0 -110 +120 -5057 fill=8 (157) \$ E21
658 0 -110 +120 -5058 fill=8 (158) \$ E22
659 0 -110 +120 -5059 fill=8 (159) \$ E23
660 0 -110 +120 -5060 fill=8 (160) \$ E24
661 0 -110 +120 -5061 fill=8 (161) \$ F1
662 0 -110 +120 -5062 fill=8 (162) \$ F2
c 663 0 -110 +120 -5063 fill=8 (163) \$ F3
c 664 0 -110 +120 -5064 fill=8 (164) \$ F4
c 665 0 -110 +120 -5065 fill=8 (165) \$ F5

666 0 -110 +120 -5066 fill=8 (166) \$ F6
667 0 -110 +120 -5067 fill=8 (167) \$ F7
668 0 -110 +120 -5068 fill=8 (168) \$ F8
669 0 -110 +120 -5069 fill=8 (169) \$ F9
670 0 -110 +120 -5070 fill=8 (170) \$ F10
671 0 -110 +120 -5071 fill=8 (171) \$ F11
672 0 -110 +120 -5072 fill=8 (172) \$ F12
673 0 -110 +120 -5073 fill=8 (173) \$ F13
674 0 -110 +120 -5074 fill=8 (174) \$ F14
675 0 -110 +120 -5075 fill=8 (175) \$ F15
676 0 -110 +120 -5076 fill=8 (176) \$ F16
677 0 -110 +120 -5077 fill=8 (177) \$ F17
678 0 -110 +120 -5078 fill=8 (178) \$ F18
679 0 -110 +120 -5079 fill=8 (179) \$ F19
680 0 -110 +120 -5080 fill=8 (180) \$ F20
681 0 -110 +120 -5081 fill=8 (181) \$ F21
682 0 -110 +120 -5082 fill=8 (182) \$ F22
683 0 -110 +120 -5083 fill=8 (183) \$ F23
684 0 -110 +120 -5084 fill=8 (184) \$ F24
685 0 -110 +120 -5085 fill=8 (185) \$ F25
686 0 -110 +120 -5086 fill=8 (186) \$ F26
687 0 -110 +120 -5087 fill=8 (187) \$ F27
688 0 -110 +120 -5088 fill=8 (188) \$ F28
689 0 -110 +120 -5089 fill=8 (189) \$ F29
690 0 -110 +120 -5090 fill=8 (190) \$ F30
691 0 -110 +120 -5091 fill=6 (191) \$ G2
692 0 -110 +120 -5092 fill=8 (192) \$ G3

c 693 0 -110 +120 -5093 fill=8 (193) \$ G4
c 694 0 -110 +120 -5094 fill=8 (194) \$ G5
695 0 -110 +120 -5095 fill=8 (195) \$ G6
696 0 -110 +120 -5096 fill=8 (196) \$ G8
697 0 -110 +120 -5097 fill=8 (197) \$ G9
698 0 -110 +120 -5098 fill=8 (198) \$ G10
699 0 -110 +120 -5099 fill=8 (199) \$ G11
700 0 -110 +120 -5100 fill=8 (200) \$ G12
701 0 -110 +120 -5101 fill=8 (201) \$ G14
702 0 -110 +120 -5102 fill=8 (202) \$ G15
703 0 -110 +120 -5103 fill=6 (203) \$ G16
704 0 -110 +120 -5104 fill=8 (204) \$ G17
705 0 -110 +120 -5105 fill=8 (205) \$ G18
706 0 -110 +120 -5106 fill=6 (206) \$ G20
707 0 -110 +120 -5107 fill=8 (207) \$ G21
708 0 -110 +120 -5108 fill=8 (208) \$ G22
709 0 -110 +120 -5109 fill=8 (209) \$ G23
710 0 -110 +120 -5110 fill=6 (210) \$ G24
c 711 0 -110 +120 -5111 fill=8 (211) \$ G26
712 0 -110 +120 -5112 fill=8 (212) \$ G27
713 0 -110 +120 -5113 fill=8 (213) \$ G28
714 0 -110 +120 -5114 fill=8 (214) \$ G29
c 715 0 -110 +120 -5115 fill=8 (215) \$ G30
c 716 0 -110 +120 -5116 fill=8 (216) \$ G32 \$ Location of source
717 0 -110 +120 -5117 fill=6 (217) \$ G33 \$ Graphite
c 718 0 -110 +120 -5118 fill=8 (218) \$ G34 \$ Location of PNT
719 0 -110 +120 -5119 fill=6 (219) \$ G35 \$ Graphite

720 0 -110 +120 -5120 fill=6 (220) \$ G36

c

750 0 -110 +120 -1940 fill=96 (50) \$ Sleeve irradiator

c

c 751 0 -110 +120 -961 fill=40 (20) \$ 3L(Pb) irradiator

c

c 751 0 -110 +120 -961 fill=45 (20) \$ 3L(Cd) irradiator

c

c 752 0 -110 +120 -5118 fill=30 (218) \$ tPNT irradiator

c

c 752 0 -110 +120 -5118 fill=35 (218) \$ ePNT irradiator

c

c -----

c Lower grid plate region

c -----

1 2 -2.7 -206 +207

-211 +212 -213 +214 -215 +216

-221 +222 -223 +224 -225 +226

+5000 +5001 +5002 +5003 +5004 +5005 +5006 +5007 +5008 +5009

+5010 +5011 +5012 +5013 +5014 +5015 +5016 +5017 +5018 +5019

+5020 +5021 +5022 +5023 +5024 +5025 +5026 +5027 +5028 +5029

+5030 +5031 +5032 +5033 +5034 +5035 +5036 +5037 +5038

+5041 +5042 +5043 +5044 +5045 +5046 +5048 +5049

+5050 +5051 +5052 +5053 +5054 +5055 +5056 +5057 +5058 +5059

+5060 +5061 +5062 +5066 +5067 +5068 +5069

+5070 +5071 +5072 +5075 +5076 +5077 +5078 +5079

+5080 +5081 +5082 +5083 +5084 +5085 +5086 +5087 +5088 +5089

+5090 +5091 +5092 +5095 +5096 +5097 +5098 +5099

+5100 +5102 +5103 +5104 +5105 +5106 +5107 +5108 +5109

+5110 +5112 +5113 +5114 +5117 +5118 +5119

+5120

+5101

+1963 +1964 +1965 +1966 \$ Mapping experiment

+1940 \$ 6L

+5047 +5073 +5074 \$ Elements in 3L

c +5111 +5115

c +5039 +5040 +5063 +5064 +5065 +5093 +5094 \$ Elements in 6L

c +961 \$ 3L

c +5118 \$ PNT

c

c -----

c Upper grid plate region

c -----

2 2 -2.7 -203 -201 +202

+5000 +5001 +5002 +5003 +5004 +5005 +5006 +5007 +5008 +5009

+5010 +5011 +5012 +5013 +5014 +5015 +5016 +5017 +5018 +5019

+5020 +5021 +5022 +5023 +5024 +5025 +5026 +5027 +5028 +5029

+5030 +5031 +5032 +5033 +5034 +5035 +5036 +5037 +5038

+5041 +5042 +5043 +5044 +5045 +5046 +5048 +5049

+5050 +5051 +5052 +5053 +5054 +5055 +5056 +5057 +5058 +5059

+5060 +5061 +5062 +5066 +5067 +5068 +5069

+5070 +5071 +5072 +5075 +5076 +5077 +5078 +5079

+5080 +5081 +5082 +5083 +5084 +5085 +5086 +5087 +5088 +5089

+5090 +5091 +5092 +5095 +5096 +5097 +5098 +5099

+5100 +5102 +5103 +5104 +5105 +5106 +5107 +5108 +5109

+5110 +5112 +5113 +5114 +5117 +5118 +5119

+5120

+5101

+1963 +1964 +1965 +1966 \$ Mapping experiment

+1940 \$ 6L

+5047 +5073 +5074 \$ Elements in 3L

c +5111 +5115

c +5039 +5040 +5063 +5064 +5065 +5093 +5094 \$ Elements in 6L

c +961 \$ 3L

c +5118 \$ PNT

c

c -----

c Reactor core structure

c -----

c Inner core shroud

c -----

10 2 -2.7 -300 +302 -303 +202 \$ Alignment ring

11 2 -2.7 -300 -202 +352 \$ Alignment ring

(+231: -232: +241: -242:

+233: -234: +243: -244:

+235: -236: +245: -246)

12 2 -2.7 +305 -306 +307 \$ Shroud load ring

(-311 +312 -321 +322

-313 +314 -323 +324

-315 +316 -325 +326)

13 2 -2.7 -301 -352 +304 \$ Alignment ring

(+331: -332: +341: -342:

+333: -334: +343: -344:

+335: -336: +345: -346)

14 2 -2.7 +231 -331 -233 +236 \$ Reflector plate
-352 +306

15 2 -2.7 -232 +332 +234 -235 \$ Reflector plate
-352 +306

16 2 -2.7 +241 -341 -343 -345 \$ Reflector, bp3
-352 +306 +363

17 2 -2.7 -242 +342 +344 +346 \$ Reflector plate
-352 +306

18 2 -2.7 +233 -333 -331 -343 \$ Reflector plate
-352 +306

19 2 -2.7 -234 +334 +332 +344 \$ Reflector plate
-352 +306

20 2 -2.7 +235 -335 +332 -345 \$ Reflector plate
-352 +306

21 2 -2.7 -236 +336 -331 +346 \$ Reflector plate
-352 +306

22 2 -2.7 +243 -343 -241 -233 \$ Reflector plate
-352 +306

23 2 -2.7 -244 +344 +242 +234 \$ Reflector plate
-352 +306

24 2 -2.7 +245 -345 -241 -235 \$ Reflector plate
-352 +306

25 2 -2.7 -246 +346 +242 +236 \$ Reflector plate
-352 +306

26 2 -2.7 +241 -363 +364 -360 \$ Reflector BP3

27 2 -2.7 -361 +362 -100 \$ Reflector BP1&5

c

c -----

c Reflector outer shroud structure

c -----

30 2 -2.7 -355 +361 \$ Reflector cylin

-350 +351 -352 +353

31 2 -2.7 +355 +363 \$ Reflector cylin

-350 +351 -352 +353

32 2 -2.7 -370 +371 -372 +373 \$ Cylinder, top

33 2 -2.7 -374 -375 +376 \$ Cylinder, bot

(+331: -332: +341: -342:

+333: -334: +343: -344:

+335: -336: +345: -346)

34 2 -2.7 -370 +374 -375 +377 \$ Reflector edge ring

35 2 -2.7 -352 -371 +380 +381 \$ Reflector RSR unit

36 2 -2.7 -380 +300 +381 -382 \$ Reflector RSR unit

37 2 -2.7 -352 +301 -300 +381 \$ Reflector RSR unit

38 1 -1.0 +370 -351 -377 +120 \$ Edge ring error

c

c -----

c Reflector graphite moderator

c -----

40 4 -1.60 -400 +401 -402 +403 \$ Reflector graphite

41 4 -1.60 -400 -403 +375 -404 +361

(+411: -412: +421: -422:

+413: -414: +423: -424:
 +415: -416: +425: -426)
 #(-361 +405) \$ Graphite, bp1&5
 42 4 -1.60 (-400 -403 +375 +404 +363
 (+411: -412: +421: -422:
 +413: -414: +423: -424:
 +415: -416: +425: -426))
 #(-406 +408) #(-407 +409) \$ Graphite, bp3
 43 8 -1.15e-3 (+371 -351 -373 +403) #40 \$ Graphite void?????
 44 8 -1.15e-3 (-351 -403 +375 -404 +361
 (+331: -332: +341: -342:
 +333: -334: +343: -344:
 +335: -336: +345: -346)) #41 \$ graphite void
 45 8 -1.15e-3 (-351 -403 +375 +404 +363
 (+331: -332: +341: -342:
 +333: -334: +343: -344:
 +335: -336: +345: -346)) #42 \$ graphite void
 46 8 -1.15e-3 -304 +403 -301
 (+331: -332: +341: -342:
 +333: -334: +343: -344:
 +335: -336: +345: -346) \$ graphite void
 47 8 -1.15e-3 +301 -371 +403 -381 \$ graphite void
 c
 c -----
 c Pool coolant water
 c -----
 50 1 -1.0 -203 +201 -110 \$ Above upper grid plate

+5000 +5001 +5002 +5003 +5004 +5005 +5006 +5007 +5008 +5009
+5010 +5011 +5012 +5013 +5014 +5015 +5016 +5017 +5018 +5019
+5020 +5021 +5022 +5023 +5024 +5025 +5026 +5027 +5028 +5029
+5030 +5031 +5032 +5033 +5034 +5035 +5036 +5037 +5038
+5041 +5042 +5043 +5044 +5045 +5046 +5048 +5049
+5050 +5051 +5052 +5053 +5054 +5055 +5056 +5057 +5058 +5059
+5060 +5061 +5062 +5066 +5067 +5068 +5069
+5070 +5071 +5072 +5075 +5076 +5077 +5078 +5079
+5080 +5081 +5082 +5083 +5084 +5085 +5086 +5087 +5088 +5089
+5090 +5091 +5092 +5095 +5096 +5097 +5098 +5099
+5100 +5102 +5103 +5104 +5105 +5106 +5107 +5108 +5109
+5110 +5112 +5113 +5114 +5117 +5118 +5119

+5120

+5101

+1940 \$ 6L

+5047 +5073 +5074 \$ Elements in 3L

c +5111 +5115

c +5039 +5040 +5063 +5064 +5065 +5093 +5094 \$ Elements in 6L

c +961 \$ 3L

c +5118 \$ PNT

c

51 1 -1.0 +203 -302 +202 -110 \$ Upper gridplate

52 1 -1.0 +302 -300 +303 -110 \$ Upper gridplate

53 1 -1.0 -305 -306 +307 \$ Lower gridplate

+5000 +5001 +5002 +5003 +5004 +5005 +5006 +5007 +5008 +5009
+5010 +5011 +5012 +5013 +5014 +5015 +5016 +5017 +5018 +5019
+5020 +5021 +5022 +5023 +5024 +5025 +5026 +5027 +5028 +5029

+5030 +5031 +5032 +5033 +5034 +5035 +5036 +5037 +5038
+5041 +5042 +5043 +5044 +5045 +5046 +5048 +5049
+5050 +5051 +5052 +5053 +5054 +5055 +5056 +5057 +5058 +5059
+5060 +5061 +5062 +5066 +5067 +5068 +5069
+5070 +5071 +5072 +5075 +5076 +5077 +5078 +5079
+5080 +5081 +5082 +5083 +5084 +5085 +5086 +5087 +5088 +5089
+5090 +5091 +5092 +5095 +5096 +5097 +5098 +5099
+5100 +5102 +5103 +5104 +5105 +5106 +5107 +5108 +5109
+5110 +5112 +5113 +5114 +5117 +5118 +5119
+5120
+5101
+1940 \$ 6L
+5047 +5073 +5074 \$ Elements in 3L

c +5111 +5115

c +5039 +5040 +5063 +5064 +5065 +5093 +5094 \$ Elements in 6L

c +961 \$ 3L

c +5118 \$ PNT

c

54 1 -1.0 -307 +120 \$ Lower gridplate

(-311 +312 -321 +322

-313 +314 -323 +324

-315 +316 -325 +326)

+5000 +5001 +5002 +5003 +5004 +5005 +5006 +5007 +5008 +5009

+5010 +5011 +5012 +5013 +5014 +5015 +5016 +5017 +5018 +5019

+5020 +5021 +5022 +5023 +5024 +5025 +5026 +5027 +5028 +5029

+5030 +5031 +5032 +5033 +5034 +5035 +5036 +5037 +5038

+5041 +5042 +5043 +5044 +5045 +5046 +5048 +5049

+5050 +5051 +5052 +5053 +5054 +5055 +5056 +5057 +5058 +5059

+5060 +5061 +5062 +5066 +5067 +5068 +5069

+5070 +5071 +5072 +5075 +5076 +5077 +5078 +5079

+5080 +5081 +5082 +5083 +5084 +5085 +5086 +5087 +5088 +5089

+5090 +5091 +5092 +5095 +5096 +5097 +5098 +5099

+5100 +5102 +5103 +5104 +5105 +5106 +5107 +5108 +5109

+5110 +5112 +5113 +5114 +5117 +5118 +5119

+5120

+5101

+1940 \$ 6L

+5047 +5073 +5074 \$ Elements in 3L

c +5111 +5115

c +5039 +5040 +5063 +5064 +5065 +5093 +5094 \$ Elements in 6L

c +961 \$ 3L

c +5118 \$ PNT

c

55 1 -1.0 -207 +306 \$ Lower gridplate

(-231 +232 -241 +242

-233 +234 -243 +244

-235 +236 -245 +246)

+5000 +5001 +5002 +5003 +5004 +5005 +5006 +5007 +5008 +5009

+5010 +5011 +5012 +5013 +5014 +5015 +5016 +5017 +5018 +5019

+5020 +5021 +5022 +5023 +5024 +5025 +5026 +5027 +5028 +5029

+5030 +5031 +5032 +5033 +5034 +5035 +5036 +5037 +5038

+5041 +5042 +5043 +5044 +5045 +5046 +5048 +5049

+5050 +5051 +5052 +5053 +5054 +5055 +5056 +5057 +5058 +5059

+5060 +5061 +5062 +5066 +5067 +5068 +5069

+5070 +5071 +5072 +5075 +5076 +5077 +5078 +5079

+5080 +5081 +5082 +5083 +5084 +5085 +5086 +5087 +5088 +5089

+5090 +5091 +5092 +5095 +5096 +5097 +5098 +5099

+5100 +5102 +5103 +5104 +5105 +5106 +5107 +5108 +5109

+5110 +5112 +5113 +5114 +5117 +5118 +5119

+5120

+5101

+1940 \$ 6L

+5047 +5073 +5074 \$ Elements in 3L

c +5111 +5115

c +5039 +5040 +5063 +5064 +5065 +5093 +5094 \$ Elements in 6L

c +961 \$ 3L

c +5118 \$ PNT

c

56 1 -1.0 -206 +207 \$ Lower gridplate

(+211: -212: +221: -222:

+213: -214: +223: -224:

+215: -216: +225: -226)

(-231 +232 -241 +242

-233 +234 -243 +244

-235 +236 -245 +246)

57 1 -1.0 -351 +371 +372 -110 \$ Upper reflector

58 1 -1.0 -374 -376 +120 \$ Lower reflector

(+311: -312: +321: -322:

+313: -314: +323: -324:

+315: -316: +325: -326)

59 1 -1.0 +306 -376 \$ Lower reflector

(+331: -332: +341: -342:

+333: -334: +343: -344:

+335: -336: +345: -346)

(-311 +312 -321 +322

-313 +314 -323 +324

-315 +316 -325 +326)

c

c -----

c Pool coolant water

c -----

950 8 -1.15e-3 -150 +160 -165

*TRCL (-60.00 00.00 00.00 00 90 90 90 00 90) \$NP

951 8 -1.15e-3 -150 +160 -165

*TRCL (57.96 -15.53 00.00 00 90 90 90 00 90) \$NPP

952 8 -1.15e-3 -150 +160 -165

*TRCL (42.43 42.43 00.00 00 90 90 90 00 90) \$FC

60 1 -1.0 +350 -355 +361

(-100 -110 +120) #950 #951 \$ Beam ports 1&5

61 1 -1.0 +350 +355 +363

(-100 -110 +120) #950 #952

#(-406 +408) #(-407 +409) \$ Beam ports 2&4

62 1 -1.0 -363 +364 +360 -100 \$ Reflector BP3

63 1 -1.0 -350 +351 +352 -110 \$ Reflector cylinder

64 1 -1.0 -350 +351 -353 +120 \$ Reflector cylinder

65 1 -1.0 -370 +374 -377 +120 \$ Reflector edgering

66 1 -1.0 +300 -371 +303 -110 \$ RSR removal

67 2 -2.7 +370 -351 -375 +377 \$ edge ring error

68 2 -2.7 -351 +370 -372 +373 \$ edge ring error

c -----

c BP2, BP4 structure

c -----

71 2 -2.7 (-406 +430) +350 +355 -100 \$ Reflector BP2

72 2 -2.7 (-407 +440) +350 +355 -100 \$ Reflector BP4

c

c -----

c BP3 structure

c -----

73 2 -2.7 +461 -462 -464 \$ Reflector BP3

74 2 -2.7 -463 +464 +461 -100 \$ Reflector BP3

75 1 -1.0 +241 -364 -461 \$ Reflector BP3

76 1 -1.0 +463 -364 +461 -100 \$ Reflector BP3

c

c -----

c BP1, BP3, BP5 cavity

c -----

77 8 -1.15e-3 +450 -362 -451 \$ Reflector BP1

78 8 -1.15e-3 +462 -464 -453 \$ Reflector BP3

79 8 -1.15e-3 -450 -362 +455

c

c -----

c BP1, BP2, BP3, BP4, BP5 cavity

c -----

81 8 -1.15e-3 +451 -362 -100 #95 VOL=1 \$ Reflector BP1

82 8 -1.15e-3 (-430 +408) +350 -100 #96 VOL=1 \$ Reflector BP2

83 8 -1.15e-3 +453 -464 -100 #97 VOL=1 \$ Reflector BP3
84 8 -1.15e-3 (-440 +409) +350 -100 #98 VOL=1 \$ Reflector BP4
85 8 -1.15e-3 -455 -362 -100 #99 VOL=1 \$ Reflector BP5

c

95 8 -1.15e-3 -171
96 8 -1.15e-3 -172
97 8 -1.15e-3 -173
98 8 -1.15e-3 -174
99 8 -1.15e-3 -175

c

c -----

c Rotary specimen rack (RSR) unit

c -----

90 8 -1.15e-3 +300 -303 +352 -371 \$ RSR unit
91 8 -1.15e-3 +300 +304 -352 -380 \$ RSR unit
92 8 -1.15e-3 +300 -304 -380 +382 \$ RSR unit

c

c -----

c Fill universe for reactor core grid

c -----

c Graphite reflector elements, U=6

c -----

100 1 -1.0 #101 #102 #103
 #104 #105 #106 u=6
101 2 -2.7 -623 -609 +206 u=6 \$ lower fitting
102 2 -2.7 -605 -620 +621 u=6 \$ end closure
103 4 -1.60 -605 -621 +622 u=6 \$ graphite

104 2 -2.7 -605 -622 +623 u=6 \$ end closure
105 2 -2.7 +620 -609 -201 u=6 \$ upper fitting
106 2 -2.7 +605 -607 -620 +623 u=6 \$ element clad

c

c -----

c Transient control rod, U=7

c -----

110 1 -1.0 #111 #112 #113 #114

#115 #116 #117 u=7

111 2 -2.7 -500 -510 +511 u=7 \$ end plug

112 2 -2.7 -500 -511 +512 u=7 \$ spacer plug

113 6 -2.52 -500 -512 +513 u=7 \$ absorber

114 2 -2.7 -500 -513 +514 u=7 \$ spacer plug

115 8 -1.15e-3 -500 -514 +515 u=7 \$ air follower

116 3 -7.8 -500 -515 +516 u=7 \$ end plug

117 3 -7.8 +500 -502 -510 +516 u=7 \$ element clad

c

c -----

c Standard triga fuel element, U=8

c -----

c Temperature in fuel rod assumed 300 C at full power

120 1 -1.0 #121 #122 #123

#124 #125 #126

#127 #128 #129 u=8 \$ element clad

121 3 -7.8 -615 -603 +206 u=8 \$ lower fitting

122 3 -7.8 -600 -610 +611 u=8 \$ end closure

123 4 -1.60 -600 -611 +612 u=8 \$ graphite

124 5 -6.05 -600 -612 +613 +650 u=8 \$ TMP1=4.939E-8 \$ fuel

125 7 -6.49 -650 -612 +613 u=8 \$ Zr rod

126 4 -1.60 -600 -613 +614 u=8 \$ graphite

127 3 -7.8 -600 -614 +615 u=8 \$ end closure

128 3 -7.8 +610 -603 -201 u=8 \$ upper fitting

129 3 -7.8 +600 -602 -610 +615 u=8 \$ element clad

c

c -----

c Fuel follower control rods (reg, shim1, shim2), U=9

c -----

c Temperature assumed 300 C at full power

130 1 -1.0 #131 #132 #133 #134 #135

#136 #137 #138 #139 #140

#141 #142 #143 u=9

131 3 -7.8 -505 -520 +521 u=9 \$ end plug

132 8 -1.15e-3 -505 -521 +522 u=9 \$ top space

133 2 -2.7 -505 -522 +523 u=9 \$ spacer plug

134 8 -1.15e-3 -505 -523 +524 u=9 \$ void gap

135 6 -2.52 -505 -524 +525 u=9 \$ absorber, inside 505,524; outside 525,

136 2 -2.7 -505 -525 +526 u=9 \$ spacer plug

137 8 -1.15e-3 -505 -526 +527 u=9 \$ void gap

138 5 -6.05 -505 -527 +528 +550 u=9 \$ TMP1=4.939E-8 \$ fuel follower

139 7 -6.49 -550 -527 +528 u=9 \$ Zr rod

140 2 -2.7 -505 -528 +529 u=9 \$ spacer plug

141 8 -1.15e-3 -505 -529 +530 u=9 \$ bot space

142 3 -7.8 -505 -530 +531 u=9 \$ end plug

143 3 -7.8 +505 -507 -520 +531 u=9 \$ element clad

c

c -----

c Modifications and experiment components

c -----

c Pneumatic transfer system (PTS) without Cd, U=30 -JDB -4/13/2007

c -----

300 1 -1.0 #301 #302 #303

#304 #305 #306

#307 #308 U=30 \$ Water surrounding PTS

301 2 -2.7 -910 +911 +933 U=30 \$ Al transport tube

302 8 -1.15e-3 -911 +912 +933 U=30 \$ Air gap

303 2 -2.7 -912 +913 +915 U=30 \$ Al sample tube

304 8 -1.15e-3 -913 +915 #308 U=30 \$ Sample location

305 2 -2.7 -910 +934 -933 U=30 \$ Al transport tube bottom

306 2 -2.7 -912 +931 -915 U=30 \$ Al sample tube bottom

307 8 -1.15e-3 +933 -931 -912 U=30 \$ Air gap beneath sample tube

308 8 -1.15e-3 -908 +909 -907 U=30 \$ Sample location for tally

c

c -----

c Pneumatic transfer system (PTS) with Cd, U=35 -JDB -4/13/2007

c -----

350 1 -1.0 #351 #352 #353

#354 #355 #356

#357 #358 #359 #360 U=35 \$ Water surrounding PTS

351 2 -2.7 -910 +911 +933 U=35 \$ Al transport tube

352 8 -1.15e-3 -911 +914 +933 U=35 \$ Air gap

353 10 -8.65 -914 +912 +931 U=35 \$ Cd liner

354 2 -2.7 -912 +913 +915 U=35 \$ Al sample tube
 355 8 -1.15e-3 -913 +915 #360 U=35 \$ Sample location
 356 2 -2.7 -910 +934 -933 U=35 \$ Al transport tube bottom
 357 2 -2.7 -912 +931 -915 U=35 \$ Al sample tube bottom
 358 10 -8.65 -914 -931 +932 U=35 \$ Cd liner beneath sample
 359 8 -1.15e-3 +933 -932 -914 U=35 \$ Air gap beneath sample tube
 360 8 -1.15e-3 -908 +909 -907 U=35 \$ Sample location for tally

c

c -----

c 3-element irradiator with Pb, U=40

c -----

400 1 -1.0 #401 #402 #403 #404

#405 #406 #407 #408

#409 #410 u=40 \$ Water

401 2 -2.7 -920 +921 -958 +959 u=40 \$ Al outer

402 8 -1.15e-3 -921 +924 -958 +959 u=40 \$ Air gap

403 11 -11.4 -924 +922 -958 +959 u=40 \$ Pb liner

404 2 -2.7 -922 +923 -958 +959 u=40 \$ Al liner

405 8 -1.15e-3 -923 -963 +965 u=40 \$ Air in sample location

406 8 -1.15e-3 -923 -958 +963 u=40 \$ Air above sample location

407 2 -2.7 -962 -957 +958 u=40 \$ Upper end cap

408 2 -2.7 -920 -959 +960 u=40 \$ Lower end cap

409 2 -2.7 -923 -965 +966 u=40

410 11 -11.4 -923 -966 +959 u=40

c

c -----

c 3-element irradiator with Cd, U=45

c -----

450 1 -1.0 #451 #452 #453 #454

#455 #456 #457 #458

#459 #460 U=45 \$ Water

451 2 -2.7 -920 +921 -958 +959 U=45 \$ Al outer

452 2 -2.7 -922 +923 -958 +959 U=45 \$ Al liner

453 10 -8.65 +922 -924 -958 +959 U=45 \$ Cd liner

454 8 -1.15e-3 -921 +924 -958 +959 U=45 \$ Air gap

455 8 -1.15e-3 -923 -963 +965 U=45 \$ Air in sample location

456 8 -1.15e-3 -923 -958 +963 u=45 \$ Air above sample location

457 2 -2.7 -962 -957 +958 u=45 \$ Upper end cap

458 2 -2.7 -920 -959 +960 u=45 \$ Lower end cap

459 2 -2.7 -923 -965 +966 u=45

460 10 -8.65 -923 -966 +959 u=45

c

c -----

c 3-element irradiator (unlined), U=50

c -----

490 8 -1.15e-3 #491 #492 #493 #494 U=50 \$

491 2 -2.7 -922 +923 -950 +955 U=50 \$ T3 can cylinder

492 2 -2.7 +922 -924 -950 +955 U=50 \$ T3 can liner

493 2 -2.7 -923 +950 -951 U=50 \$ T3 can upper

494 2 -2.7 -923 -955 +956 U=50 \$ T3 can lower

c

c -----

c Water cells for mapping experiment, u=101

c -----

515 1 -1.0 #516 u=101

516 1 -1.0 -754 +782 -750 u=101

c

c -----

c Large irradiator with cadmium sleeve, u=96

c -----

811 1 -1.0 #812 #813 #814 #815

#816 #817 #818 #819

#820 #821 #822 u=96 \$ Water outside of 7L

c

812 2 -2.7 -1941 +1942 +1959 -1960 u=96 \$ Al clad outer, sleeve

813 11 -11.4 -1942 +1943 +1959 -1960 u=96 \$ Pb liner, sleeve

814 2 -2.7 -1943 +1944 +1959 -1960 u=96 \$ Al clad inner, sleeve

c

815 2 -2.7 -1945 +1946 -957 +965 u=96 \$ Al clad, can

816 21 -2.7 -1946 +1947 -957 +965 u=96 \$ Al-B liner, can

817 8 -1.15e-3 -1947 -963 +965 u=96 \$ Air in sample location, can

818 8 -1.15e-3 -1947 -958 +963 u=96 \$ Air above sample, can

c

819 2 -2.7 -1941 +1944 -1961 +1960 u=96 \$ Upper end fitting, sleeve

820 2 -2.7 -1941 +1944 -1959 +1956 u=96 \$ Lower end fitting, sleeve

c

821 2 -2.7 -1945 -957 +958 u=96 \$ Upper end fitting, can

822 2 -2.7 -1945 -965 +1956 u=96 \$ Lower end fitting, can

c

c -----

c 1-inch detector

c -----

1740 1 -1.0 #1741 #1742 U=81 \$ element clad

1741 8 -1.15e-3 -638 -639 +640 #1742 U=81

1742 8 -1.15e-3 -638 -641 +642 U=81 \$ flux tally for 1" dia FC

c

c -----

c Central thimble (CT), u=82 -JDB

c -----

1750 1 -1.0 #1751 #1752 u=82

1751 2 -2.7 -442 +443 +207 u=82

1752 1 -1.0 -446 +447 -445 u=82

c

c -----

c Photon Radial Profile Holes

c -----

1800 1 -1.0 -2000

1801 1 -1.0 -2001

1802 1 -1.0 -2002

1803 1 -1.0 -2003

1804 1 -1.0 -2004

1805 1 -1.0 -2005

1806 1 -1.0 -2006

c -----

c Tube cell for my test (Alex Zhou 2009)

c -----

9001 9910 -1 -9001 \$ solution inside container

9002 99 -.93 -9002 +9001 \$ container of polyethylene

c 9012 1 -1 -111 +121 -9010 +9002 \$ cell of surface source

9003 1 -1 -110 +120 -9003 +9002 \$ outside container, inside surface 602,
water in between

9004 2 -2.7 -110 +120 -9004 +9003 \$ shell

9005 1 -1 -110 +120 -5118 +9004 \$ out shell

c

c -----

c Outside world

c -----

2999 0 +100: +110: -120

c

c

c below are a few references of surfaces used for the cell

c -----

c 718 0 -110 +120 -5118 fill=8 (218) \$ G34 \$ Location of PNT

c tr218 +19.59102 +11.31062 0.0 \$ G34

c 5118 c/z +19.59102 +11.31062 +1.91135 \$ Upper grid plate hole, G34

c

c 9001 rcc +19.59102 +11.31062 0.05 0 0 1.5 0.5 \$ sample space inside
container

c 9002 rcc +19.59102 +11.31062 0 0 0 1.6 0.55 \$ container of polyethylene

c 9003 c/z +19.59102 +11.31062 +1.816 \$ assembly for G34

c 9004 c/z +19.59102 +11.31062 +1.867 \$ out shell

c 9010 c/z +19.59102 +11.31062 +1.5 \$ surface source bound

c -----

c End of Cell Card Specification

c -----

c -----

c Beginning of Surface Card Specification

c -----

c Hexagonal cell lattice surfaces

c -----

101 PX +2.17678 \$ Fuel lattice hex-prism

102 PX -2.17678 \$ Fuel lattice hex-prism

103 P +1 1.73205 0 +4.35356 \$ Fuel lattice hex-prism

104 P +1 1.73205 0 -4.35356 \$ Fuel lattice hex-prism

105 P -1 1.73205 0 +4.35356 \$ Fuel lattice hex-prism

106 P -1 1.73205 0 -4.35356 \$ Fuel lattice hex-prism

107 CZ +2.51353 \$ Maximum lattice diagonal radius

c

108 py 5.65531

109 py -5.65531

c

c -----

c Axial and radial domain

c -----

100 CZ +75

110 PZ +75 \$ Upper bound

111 pz +3.3 \$ Upper cap of surface source

120 PZ -75 \$ Lower bound

121 PZ -1.7 \$ Lower cap of surface source

150 CZ +5.08 \$ Detector Cylinder

160 PZ +10 \$ Detector Lower

165 PZ +30 \$ Detector Upper

c

171 s 60.000 -36.000 -6.985 2.5 \$ bp1

172 s 60.000 36.000 -6.985 2.5 \$ bp2

173 s 0.000 70.000 -6.985 2.5 \$ bp3

174 s -60.000 36.000 -6.985 2.5 \$ bp4

175 s -60.000 -36.000 -6.985 2.5 \$ bp5

c

c -----

c Reactor core grid plate surfaces

c -----

200 CZ 1.91135 \$ Grid plate element holes

201 PZ +32.3850 \$ Upper grid plate region

202 PZ +30.7975 \$ Upper grid plate region

203 CZ 27.6225 \$ Upper grid plate diameter -effective core diameter

205 CZ 1.5875 \$ Grid plate coolant holes

206 PZ -33.17875 \$ Lower grid plate region

207 PZ -36.35375 \$ Lower grid plate region

211 PX +26.1216 \$ Lower grid plate edge

212 PX -26.1216 \$ Lower grid plate edge

213 P +1 0.57735 0 +29.0240 \$ Lower grid plate edge

214 P +1 0.57735 0 -29.0240 \$ Lower grid plate edge

215 P -1 0.57735 0 +29.0240 \$ Lower grid plate edge

216 P -1 0.57735 0 -29.0240 \$ Lower grid plate edge

221 PY +25.1360 \$ Lower grid plate edge

222 PY -25.1360 \$ Lower grid plate edge

223 P +1 1.73205 0 +52.2432 \$ Lower grid plate edge

224 P +1 1.73205 0 -52.2432 \$ Lower grid plate edge

225 P -1 1.73205 0 +52.2432 \$ Lower grid plate edge
226 P -1 1.73205 0 -52.2432 \$ Lower grid plate edge
231 PX +26.6700 \$ Core shroud inside surface
232 PX -26.6700 \$ Core shroud inside surface
233 P +1 0.57735 0 +29.2100 \$ Core shroud inside surface
234 P +1 0.57735 0 -29.2100 \$ Core shroud inside surface
235 P -1 0.57735 0 +29.2100 \$ Core shroud inside surface
236 P -1 0.57735 0 -29.2100 \$ Core shroud inside surface
241 PY +25.4000 \$ Core shroud inside surface
242 PY -25.4000 \$ Core shroud inside surface
243 P +1 1.73205 0 +54.9275 \$ Core shroud inside surface
244 P +1 1.73205 0 -54.9275 \$ Core shroud inside surface
245 P -1 1.73205 0 +54.9275 \$ Core shroud inside surface
246 P -1 1.73205 0 -54.9275 \$ Core shroud inside surface

c

c -----

c Core structure surfaces

c -----

c Reflector inner shroud

c -----

300 CZ 30.083125 \$ Grid plate alignment ring
301 CZ 29.765625 \$ Grid plate alignment ring
302 CZ 27.9400 \$ Grid plate alignment ring
303 PZ +33.9725 \$ Grid plate alignment ring
304 PZ +26.3525 \$ Grid plate alignment ring

c

c -----

c Shroud load ring

c -----

305 CZ 27.9400 \$ Reflector shroud load ring \$ 24.7650

306 PZ -37.30625 \$ Reflector shroud load ring

307 PZ -39.52875 \$ Reflector shroud load ring

c

311 PX +29.2100 \$ Reflector shroud support

312 PX -29.2100 \$ Reflector shroud support

313 P +1 0.57735 0 +32.385 \$ Reflector shroud support

314 P +1 0.57735 0 -32.385 \$ Reflector shroud support

315 P -1 0.57735 0 +32.385 \$ Reflector shroud support

316 P -1 0.57735 0 -32.385 \$ Reflector shroud support

321 PY +27.9400 \$ Reflector shroud support

322 PY -27.9400 \$ Reflector shroud support

323 P +1 1.73205 0 +59.3725 \$ Reflector shroud support

324 P +1 1.73205 0 -59.3725 \$ Reflector shroud support

325 P -1 1.73205 0 +59.3725 \$ Reflector shroud support

326 P -1 1.73205 0 -59.3725 \$ Reflector shroud support

c

331 PX +27.3050 \$ Core shroud plate exterior

332 PX -27.3050 \$ Core shroud plate exterior

333 P +1 0.57735 0 +29.8450 \$ Core shroud plate exterior

334 P +1 0.57735 0 -29.8450 \$ Core shroud plate exterior

335 P -1 0.57735 0 +29.8450 \$ Core shroud plate exterior

336 P -1 0.57735 0 -29.8450 \$ Core shroud plate exterior

341 PY +26.0350 \$ Core shroud plate exterior

342 PY -26.0350 \$ Core shroud plate exterior

343 P +1 1.73205 0 +56.5150 \$ Core shroud plate exterior

344 P +1 1.73205 0 -56.5150 \$ Core shroud plate exterior

345 P -1 1.73205 0 +56.5150 \$ Core shroud plate exterior

346 P -1 1.73205 0 -56.5150 \$ Core shroud plate exterior

c

c -----

c Reflector outer shroud

c -----

350 CZ +54.76875 \$ Reflector outer shroud

351 CZ +53.49875 \$ Reflector outer shroud

352 PZ +28.8925 \$ Outer shroud upper edge

353 PZ -32.0675 \$ Outer shroud lower edge

355 PY 0.0 \$ Core shroud section plane

c

c -----

c Reflector beam ports

c -----

360 PY +55.5625 \$ Radial penetrating beam port

361 C/X -35.2552 -6.985 7.62 \$ Tangential thru beam port

362 C/X -35.2552 -6.985 6.9088 \$ Tangential thru beam port

363 C/Y 0.0 -6.985 10.160 \$ Radial penetrating beam port

364 C/Y 0.0 -6.985 9.525 \$ Radial penetrating beam port

c

370 CZ 53.3400 \$ Reflector top shroud

371 CZ 37.4650 \$ Reflector top shroud

372 PZ +29.5275 \$ Reflector top shroud

373 PZ +28.2575 \$ Reflector top shroud

374 CZ 52.0700 \$ Reflector inner shroud base

375 PZ -27.9400 \$ Reflector inner shroud base

376 PZ -29.5275 \$ Reflector inner shroud base

377 PZ -36.8300 \$ Reflector shroud edge ring

c

c -----

c RSR experiment system

c -----

380 CZ +37.1475 \$ RSR cavity outer ring

381 PZ +6.9850 \$ RSR cavity base

382 PZ +7.3025 \$ RSR cavity base

c

c -----

c Graphite reflector surfaces

c -----

400 CZ 53.0225 \$ Graphite reflector outer radius

401 CZ 37.7825 \$ Graphite reflector inner radius

402 PZ 27.6225 \$ Graphite reflector upper section

403 PZ 6.3500 \$ Graphite reflector section plane

404 PY -20.32 \$ Graphite reflector section plane

405 PY -35.2552 \$ Beam port penetration

c C/Y 0.0 -6.985 10.160 \$ Radial penetrating beam port, bp3

c C/X -35.2552 -6.985 7.62 \$ Tangential thru beam port, bp1&5

406 2 CY 7.62 \$ Tangential beam port, bp2

407 4 CY 7.62 \$ Radial beam port, bp4

408 2 PY 0.0 \$ Tangential beam port, bp2

409 4 PY 0.0 \$ Radial beam port, bp4

411 PX +27.78125 \$ Graphite inner surface
 412 PX -27.78125 \$ Graphite inner surface
 413 P +1 0.57735 0 +31.00875 \$ Graphite inner surface +1
 414 P +1 0.57735 0 -31.00875 \$ Graphite inner surface +1
 415 P -1 0.57735 0 +31.00875 \$ Graphite inner surface +1
 416 P -1 0.57735 0 -31.00875 \$ Graphite inner surface +1
 421 PY +26.431875 \$ Graphite inner surface
 422 PY -26.431875 \$ Graphite inner surface
 423 P +1 1.73205 0 +57.30875 \$ Graphite inner surface +1
 424 P +1 1.73205 0 -57.30875 \$ Graphite inner surface +1
 425 P -1 1.73205 0 +57.30875 \$ Graphite inner surface +1
 426 P -1 1.73205 0 -57.30875 \$ Graphite inner surface +1

c

430 2 CY 6.9088 \$ Tangential beam port, bp2
 440 4 CY 6.9088 \$ Radial beam port, bp4
 450 PX 0.0 \$ BP1&5 origin

c

c -----

c Central thimble -JLP

c -----

442 CZ 1.50 \$ Central thimble guide rod OD
 443 CZ 1.415 \$ Central thimble guid rod ID
 444 CZ 1.25 \$ Central thimble sample holder OD
 445 CZ 1.185 \$ Central thimble sample holder ID
 446 PZ 2.5 \$ Central thimble upper sample hodler
 447 PZ -2.5 \$ Central thibmle lower sample holder

c beam port tally surfaces bp1&5 and bp3

451 PX +10.16 \$ BP1

453 PY +40.90 \$ BP3

455 PX -10.16 \$ BP5

c pool structure pipe, bp3

461 PY +25.600 \$ Radial penetrating beam port, bp3

462 PY +26.235 \$ Radial penetrating beam port, bp3

463 C/Y 0.0 -6.985 7.62 \$ Radial penetrating beam port, bp3

464 C/Y 0.0 -6.985 6.9088 \$ Radial penetrating beam port, bp3

c

c -----

c Control element surfaces

c -----

c data for transient rod

500 CZ 1.5113 \$ Control element -absorber surface, radius

502 CZ 1.5875 \$ Control element -clad outer surface

505 CZ 1.6637 \$ Control element -absorber surface, radius

507 CZ 1.7145 \$ Control element -clad outer surface

c

510 7 PZ +24.765 \$ Control element -element plug, end

511 7 PZ +24.13 \$ Control element -magneform plug, upper

512 7 PZ +19.05 \$ Control element -absorber surface,length/2

513 7 PZ -19.05 \$ Control element -absorber surface,length/2

514 7 PZ -21.59 \$ Control element -magneform plug, lower

515 7 PZ -70.8025 \$ Control element -air follower section

516 7 PZ -72.7075 \$ Control element -element plug, end

c

c data for shim 1, 2 & regulating rod

c

c 517 pz +75 \$

c 518 pz -75 \$

c 519 cz 1.5875 \$ repeat of 502

c 532 cz 1.7145 \$ repeat of 507

c

c lower control rod by 10 unit to reach keff=1

c

520 7 PZ +24.925 \$ Control element -element plug, end

521 7 PZ +21.115 \$ Control element -void gap

522 7 PZ +10.6375 \$ Control element -magneform plug, upper

523 7 PZ +9.3675 \$ Control element -void gap

524 7 PZ +9.05 \$ Control element -absorber surface,length/2

525 7 PZ -29.05 \$ Control element -absorber surface,length/2

526 7 PZ -30.32 \$ Control element -magneform plug, lower

527 7 PZ -30.955 \$ Control element -void gap

528 7 PZ -69.055 \$ Control element -fuel follower section

529 7 PZ -71.595 \$ Control element -void gap

530 7 PZ -84.93 \$ Control element -magneform plug, bottom

531 7 PZ -84.99 \$ Control element -element plug, end

c

550 CZ 0.28575 \$ Zirconium rod

c

c -----

c Fuel and moderator element surfaces

c -----

600 CZ 1.816 \$ Fuel element -fuel region surface, radius

602 CZ 1.867 \$ Fuel element -clad outer surface
603 CZ 1.5306 \$ Fuel -adapter effective radius, lower
604 CZ 1.9426 \$ Fuel -adapter effective radius, upper
605 CZ 1.816 \$ Graphite element -element surface, radius
606 CZ 1.867 \$ Graphite element -clad outer surface
607 CZ 1.867 \$ Graphite element -clad outer surface
608 CZ 1.9426 \$ Graphite -adapter effective radius, upper
609 CZ 1.5306 \$ Graphite -adapter effective radius, lower

c

610 PZ +28.5877 \$ Fuel element -element end region, upper
611 PZ +27.7368 \$ Fuel element -graphite end region, upper
612 PZ +19.05 \$ Fuel element -fuel surface, length/2
613 PZ -19.05 \$ Fuel element -fuel surface, length/2
614 PZ -27.7368 \$ Fuel element -graphite end region, lower
615 PZ -28.5877 \$ Fuel element -element end region, lower

c

620 PZ +28.5877 \$ Graphite element -element end, upper
621 PZ +27.7368 \$ Graphite element -graphite end, upper
622 PZ -27.7368 \$ Graphite element -graphite end, lower
623 PZ -28.5877 \$ Graphite element -element end, lower

c

635 PZ 15.24 \$ Flux Tally
636 PZ -15.24 \$ Flux Tally
637 CZ 0.4 \$ Flux Tally hole for the KSU detector
638 CZ 1.27
639 PZ 7.7851
640 PZ -7.7851

641 PZ 6.35

642 PZ -6.35

c

650 CZ 0.28575 \$ Zirconium rod

c

660 CZ 1.5306 \$ Element adapter effective radius

661 CZ 1.867 \$ Element clad outer surface

662 PZ +32.3850 \$ Upper grid plate, top

663 PZ +28.5877 \$ Element end region, upper

664 PZ -28.5877 \$ Element end region, lower

665 PZ -33.17875 \$ Lower grid plate, top

666 cz 1.91135 \$ Upper grid plate holes

c

c -----

c Boundaries for large irradiator

c -----

701 PX +8.70712

703 PX +10.8839

708 PX +19.59102

710 PX 21.7678

712 PX 19.59102

717 PX 10.8839

702 P -1 1.73205 0 -26.12136

704 P -1 1.73205 0 -21.7678

705 P 1 1.73205 0 4.35356

706 P -1 1.73205 0 -26.12136

707 P 1 1.73205 0 8.70712

709 P 1 1.73205 0 4.35356
711 P -1 1.73205 0 -43.5356
713 P -1 1.73205 0 -47.88916
714 P 1 1.73205 0 -13.06068
715 P -1 1.73205 0 -43.5356
716 P 1 1.73205 0 -17.41424
718 P 1 1.73205 0 -13.06068

c

c -----

c Reactor core modifications

c -----

c Center tube irradiations

c -----

900 CZ 1.905 \$ Center tube outer radius
901 CZ 1.69418 \$ Center tube inner radius
905 CZ 1.5 \$ Sample radius
907 PZ +0.5 \$ Sample length
908 CZ 0.5 \$ Sample radius (PTS)
909 PZ -0.5 \$ Sample length

c

c -----

c PNT tube dimensions

c -----

910 CZ +1.74625 \$ Al transport tube outer radius
911 CZ +1.53543 \$ Al transport tube inner radius
912 CZ +1.11125 \$ Al sample tube outer radius
913 CZ +0.86995 \$ Al sample tube inner radius

914 CZ +1.16205 \$ Cd two layer liner
915 PZ -2.07645 \$ PTS sample stop
916 PZ -18.89125 \$ Cd absorber end
917 PZ -21.1264591 \$ Cd absorber disk, upper edge
918 PZ -21.17725 \$ Cd absorber disk, lower edge
919 PZ -30.32125 \$ PTS bottom section
931 PZ -2.94775 \$ Al sample tube bottom
932 PZ -2.99855 \$ Bottom of Cd liner
933 PZ -3.37193 \$ Top of Al transport tube
934 PZ -3.58275 \$ Bottom of Al transport tube

c

c -----

c 3-element irradiator with Cd or Pb

c -----

c Reference to lower grid plate -33.17875

920 CZ +2.38125 \$ Al can outer radius
921 CZ +2.23393 \$ Al can inner radius
922 CZ +2.06375 \$ Al sleeve outer radius
923 CZ +1.93929 \$ Al sleeve inner radius
924 CZ +2.16535 \$ Cd liner outer radius
c 930 CZ +0.47625 \$ Al structure rod
c 940 PZ -30.xxxx \$ Al bearing section
950 PZ +2.54 \$ Al upper end cap
951 PZ +2.5908 \$ Al upper end cap
955 PZ -2.54 \$ Al lower end cap
956 PZ -2.5908 \$ Al lower end cap

c

957 pz +99.82125 \$ Al upper end cap, top
958 pz +96.82125 \$ Al upper end cap, bottom
963 pz +30.7975 \$ Bottom of upper grid plate
959 pz -26.19375 \$ Al lower end cap, top
960 pz -31.27385 \$ Al lower end cap, bottom
962 cz +3.00000

c

961 c/z -15.23746 -8.79856 +3.0099

c

965 pz -25.55875 \$ Top of Al in Al sleeve
966 pz -26.09215 \$ Top of Cd liner in sleeve
967 pz -26.19375 \$ Top of lower end cap

c

c -----

c Large irradiator surfaces

c -----

1920 cz +4.35385 \$ Al can outer radius
1921 cz +4.19510 \$ Al can inner radius
1922 cz +4.03635 \$ Al sleeve outer radius
1923 cz +3.91189 \$ Al sleeve inner radius
1924 cz +4.13795 \$ Cd liner outer radius
1925 cz +5.08254

c

1950 pz +32.3850 \$ Al upper end cap
1951 pz +32.22625 \$ Al upper end cap
1955 pz -33.02 \$ Al lower end cap
1956 pz -33.17875 \$ Al lower end cap

c

1957 pz +58.26125

1958 pz +58.89625

1959 pz -30.63875

1960 pz +60.80125

1961 pz +63.34125

c

c -----

c Large irradiator surfaces with cadmium sleeve

c -----

1940 c/z 15.23746 -11.31062 5.27939 \$ Center of irradiator

c

1941 cz 4.91998

1942 cz 4.60248

1943 cz 3.81

1944 cz 3.4925

1945 cz 3.175

1946 cz 2.8575

1947 cz 2.6575

c

c -----

c Surfaces for flux mapping with Ni wire -JDB

c -----

1963 c/z 2.17678 -1.2573 +0.16 \$ A

1964 c/z 15.23746 -1.2573 +0.16 \$ K

1965 c/z 19.59102 -1.2573 +0.16 \$ L

1966 c/z 23.94458 -1.2573 +0.16 \$ M

c

750 cz 0.15875 \$ Keep! 7/12/2006

751 cz 0.16 \$ Keep! 7/12/2006

754 pz 32.385 \$ Keep! 7/12/2006

782 pz -36.35375 \$ Keep! 7/12/2006

c

c -----

c Photon Radial Profile Holes

c -----

2000 s +0.0 +2.51353 +0.0 0.3175

2001 s +0.0 +5.020706 +0.0 0.3175

2002 s +0.0 +10.05412 +0.0 0.3175

2003 s +0.0 +12.56765 +0.0 0.3175

2004 s +0.0 +17.59470 +0.0 0.3175

2005 s +0.0 +20.10823 +0.0 0.3175

2006 s +0.0 +25.0 +0.0 0.3175

c

c -----

c Upper grid plate holes

c -----

5000 c/z +0.00000 +0.00000 +1.91135 \$ Upper grid plate hole, A1

5001 c/z +4.35356 +0.00000 +1.91135 \$ Upper grid plate hole, B1

5002 c/z +2.17678 -3.76936 +1.91135 \$ Upper grid plate hole, B2

5003 c/z -2.17678 -3.76936 +1.91135 \$ Upper grid plate hole, B3

5004 c/z -4.35356 +0.00000 +1.91135 \$ Upper grid plate hole, B4

5005 c/z -2.17678 +3.76936 +1.91135 \$ Upper grid plate hole, B5

5006 c/z +2.17678 +3.76936 +1.91135 \$ Upper grid plate hole, B6

5007 c/z +8.70712 +0.00000 +1.91135 \$ Upper grid plate hole, C1
5008 c/z +6.53034 -3.76936 +1.91135 \$ Upper grid plate hole, C2
5009 c/z +4.35356 -7.54126 +1.91135 \$ Upper grid plate hole, C3
5010 c/z -0.00000 -7.54126 +1.91135 \$ Upper grid plate hole, C4
5011 c/z -4.35356 -7.54126 +1.91135 \$ Upper grid plate hole, C5
5012 c/z -6.53034 -3.76936 +1.91135 \$ Upper grid plate hole, C6
5013 c/z -8.70712 +0.00000 +1.91135 \$ Upper grid plate hole, C7
5014 c/z -6.53034 +3.76936 +1.91135 \$ Upper grid plate hole, C8
5015 c/z -4.35356 +7.54126 +1.91135 \$ Upper grid plate hole, C9
5016 c/z -0.00000 +7.54126 +1.91135 \$ Upper grid plate hole, C10
5017 c/z +4.35356 +7.54126 +1.91135 \$ Upper grid plate hole, C11
5018 c/z +6.53034 +3.76936 +1.91135 \$ Upper grid plate hole, C12
5019 c/z +13.06068 +0.00000 +1.91135 \$ Upper grid plate hole, D1
5020 c/z +10.88390 -3.76936 +1.91135 \$ Upper grid plate hole, D2
5021 c/z +8.70712 -7.54126 +1.91135 \$ Upper grid plate hole, D3
5022 c/z +6.53034 -11.31062 +1.91135 \$ Upper grid plate hole, D4
5023 c/z +2.17678 -11.31062 +1.91135 \$ Upper grid plate hole, D5
5024 c/z -2.17678 -11.31062 +1.91135 \$ Upper grid plate hole, D6
5025 c/z -6.53034 -11.31062 +1.91135 \$ Upper grid plate hole, D7
5026 c/z -8.70712 -7.54126 +1.91135 \$ Upper grid plate hole, D8
5027 c/z -10.88390 -3.76936 +1.91135 \$ Upper grid plate hole, D9
5028 c/z -13.06068 +0.00000 +1.91135 \$ Upper grid plate hole, D10
5029 c/z -10.88390 +3.76936 +1.91135 \$ Upper grid plate hole, D11
5030 c/z -8.70712 +7.54126 +1.91135 \$ Upper grid plate hole, D12
5031 c/z -6.53034 +11.31062 +1.91135 \$ Upper grid plate hole, D13
5032 c/z -2.17678 +11.31062 +1.91135 \$ Upper grid plate hole, D14
5033 c/z +2.17678 +11.31062 +1.91135 \$ Upper grid plate hole, D15

5034 c/z +6.53034 +11.31062 +1.91135 \$ Upper grid plate hole, D16
5035 c/z +8.70712 +7.54126 +1.91135 \$ Upper grid plate hole, D17
5036 c/z +10.88390 +3.76936 +1.91135 \$ Upper grid plate hole, D18
5037 c/z +17.41424 +0.00000 +1.91135 \$ Upper grid plate hole, E1
5038 c/z +15.23746 -3.76936 +1.91135 \$ Upper grid plate hole, E2
5039 c/z +13.06068 -7.54126 +1.91135 \$ Upper grid plate hole, E3
5040 c/z +10.88390 -11.31062 +1.91135 \$ Upper grid plate hole, E4
5041 c/z +8.70712 -15.08252 +1.91135 \$ Upper grid plate hole, E5
5042 c/z +4.35356 -15.08252 +1.91135 \$ Upper grid plate hole, E6
5043 c/z -0.00000 -15.08252 +1.91135 \$ Upper grid plate hole, E7
5044 c/z -4.35356 -15.08252 +1.91135 \$ Upper grid plate hole, E8
5045 c/z -8.70712 -15.08252 +1.91135 \$ Upper grid plate hole, E9
5046 c/z -10.88390 -11.31062 +1.91135 \$ Upper grid plate hole, E10
5047 c/z -13.06068 -7.54126 +1.91135 \$ Upper grid plate hole, E11
5048 c/z -15.23746 -3.76936 +1.91135 \$ Upper grid plate hole, E12
5049 c/z -17.41424 +0.00000 +1.91135 \$ Upper grid plate hole, E13
5050 c/z -15.23746 +3.76936 +1.91135 \$ Upper grid plate hole, E14
5051 c/z -13.06068 +7.54126 +1.91135 \$ Upper grid plate hole, E15
5052 c/z -10.88390 +11.31062 +1.91135 \$ Upper grid plate hole, E16
5053 c/z -8.70712 +15.08252 +1.91135 \$ Upper grid plate hole, E17
5054 c/z -4.35356 +15.08252 +1.91135 \$ Upper grid plate hole, E18
5055 c/z -0.00000 +15.08252 +1.91135 \$ Upper grid plate hole, E19
5056 c/z +4.35356 +15.08252 +1.91135 \$ Upper grid plate hole, E20
5057 c/z +8.70712 +15.08252 +1.91135 \$ Upper grid plate hole, E21
5058 c/z +10.88390 +11.31062 +1.91135 \$ Upper grid plate hole, E22
5059 c/z +13.06068 +7.54126 +1.91135 \$ Upper grid plate hole, E23
5060 c/z +15.23746 +3.76936 +1.91135 \$ Upper grid plate hole, E24

5061 c/z +21.76780 +0.00000 +1.91135 \$ Upper grid plate hole, F1
5062 c/z +19.59102 -3.76936 +1.91135 \$ Upper grid plate hole, F2
5063 c/z +17.41424 -7.54126 +1.91135 \$ Upper grid plate hole, F3
5064 c/z +15.23746 -11.31062 +1.91135 \$ Upper grid plate hole, F4
5065 c/z +13.06068 -15.08252 +1.91135 \$ Upper grid plate hole, F5
5066 c/z +10.88390 -18.85188 +1.91135 \$ Upper grid plate hole, F6
5067 c/z +6.53034 -18.85188 +1.91135 \$ Upper grid plate hole, F7
5068 c/z +2.17678 -18.85188 +1.91135 \$ Upper grid plate hole, F8
5069 c/z -2.17678 -18.85188 +1.91135 \$ Upper grid plate hole, F9
5070 c/z -6.53034 -18.85188 +1.91135 \$ Upper grid plate hole, F10
5071 c/z -10.88390 -18.85188 +1.91135 \$ Upper grid plate hole, F11
5072 c/z -13.06068 -15.08252 +1.91135 \$ Upper grid plate hole, F12
5073 c/z -15.23746 -11.31062 +1.91135 \$ Upper grid plate hole, F13
5074 c/z -17.41424 -7.54126 +1.91135 \$ Upper grid plate hole, F14
5075 c/z -19.59102 -3.76936 +1.91135 \$ Upper grid plate hole, F15
5076 c/z -21.76780 +0.00000 +1.91135 \$ Upper grid plate hole, F16
5077 c/z -19.59102 +3.76936 +1.91135 \$ Upper grid plate hole, F17
5078 c/z -17.41424 +7.54126 +1.91135 \$ Upper grid plate hole, F18
5079 c/z -15.23746 +11.31062 +1.91135 \$ Upper grid plate hole, F19
5080 c/z -13.06068 +15.08252 +1.91135 \$ Upper grid plate hole, F20
5081 c/z -10.88390 +18.85188 +1.91135 \$ Upper grid plate hole, F21
5082 c/z -6.53034 +18.85188 +1.91135 \$ Upper grid plate hole, F22
5083 c/z -2.17678 +18.85188 +1.91135 \$ Upper grid plate hole, F23
5084 c/z +2.17678 +18.85188 +1.91135 \$ Upper grid plate hole, F24
5085 c/z +6.53034 +18.85188 +1.91135 \$ Upper grid plate hole, F25
5086 c/z +10.88390 +18.85188 +1.91135 \$ Upper grid plate hole, F26
5087 c/z +13.06068 +15.08252 +1.91135 \$ Upper grid plate hole, F27

5088 c/z +15.23746 +11.31062 +1.91135 \$ Upper grid plate hole, F28
5089 c/z +17.41424 +7.54126 +1.91135 \$ Upper grid plate hole, F29
5090 c/z +19.59102 +3.76936 +1.91135 \$ Upper grid plate hole, F30
5091 c/z +23.94458 -3.76936 +1.91135 \$ Upper grid plate hole, G2
5092 c/z +21.76780 -7.54126 +1.91135 \$ Upper grid plate hole, G3
5093 c/z +19.59102 -11.31062 +1.91135 \$ Upper grid plate hole, G4
5094 c/z +17.41424 -15.08252 +1.91135 \$ Upper grid plate hole, G5
5095 c/z +15.23746 -18.85188 +1.91135 \$ Upper grid plate hole, G6
5096 c/z +8.70712 -22.62124 +1.91135 \$ Upper grid plate hole, G8
5097 c/z +4.35356 -22.62124 +1.91135 \$ Upper grid plate hole, G9
5098 c/z -0.00000 -22.62124 +1.91135 \$ Upper grid plate hole, G10
5099 c/z -4.35356 -22.62124 +1.91135 \$ Upper grid plate hole, G11
5100 c/z -8.70712 -22.62124 +1.91135 \$ Upper grid plate hole, G12
5101 c/z -15.23746 -18.85188 +1.91135 \$ Upper grid plate hole, G14
5102 c/z -17.41424 -15.08252 +1.91135 \$ Upper grid plate hole, G15
5103 c/z -19.59102 -11.31062 +1.91135 \$ Upper grid plate hole, G16
5104 c/z -21.76780 -7.54126 +1.91135 \$ Upper grid plate hole, G17
5105 c/z -23.94458 -3.76936 +1.91135 \$ Upper grid plate hole, G18
5106 c/z -23.94458 +3.76936 +1.91135 \$ Upper grid plate hole, G20
5107 c/z -21.76780 +7.54126 +1.91135 \$ Upper grid plate hole, G21
5108 c/z -19.59102 +11.31062 +1.91135 \$ Upper grid plate hole, G22
5109 c/z -17.41424 +15.08252 +1.91135 \$ Upper grid plate hole, G23
5110 c/z -15.23746 +18.85188 +1.91135 \$ Upper grid plate hole, G24
5111 c/z -8.70712 +22.62124 +1.91135 \$ Upper grid plate hole, G26
5112 c/z -4.35356 +22.62124 +1.91135 \$ Upper grid plate hole, G27
5113 c/z +4.35356 +22.62124 +1.91135 \$ Upper grid plate hole, G29
5114 c/z -0.00000 +22.62124 +1.91135 \$ Upper grid plate hole, G28

5115 c/z +8.70712 +22.62124 +1.91135 \$ Upper grid plate hole, G30
5116 c/z +15.23746 +18.85188 +1.91135 \$ Upper grid plate hole, G32
5117 c/z +17.41424 +15.08252 +1.91135 \$ Upper grid plate hole, G33
5118 c/z +19.59102 +11.31062 +1.91135 \$ Upper grid plate hole, G34
5119 c/z +21.76780 +7.54126 +1.91135 \$ Upper grid plate hole, G35
5120 c/z +23.94458 +3.76936 +1.91135 \$ Upper grid plate hole, G36

c -----

c Cut planes for tallies

c -----

6000 pz +32
6001 pz +31
6002 pz +30
6003 pz +29
6004 pz +28
6005 pz +27
6006 pz +26
6007 pz +25
6008 pz +24
6009 pz +23
6010 pz +22
6011 pz +21
6012 pz +20
6013 pz +19
6014 pz +18
6015 pz +17
6016 pz +16
6017 pz +15

6018 pz +14

6019 pz +13

6020 pz +12

6021 pz +11

6022 pz +10

6023 pz +9

6024 pz +8

6025 pz +7

6026 pz +6

6027 pz +5

6028 pz +4

6029 pz +3

6030 pz +2

6031 pz +1

6032 pz +0

6033 pz -1

6034 pz -2

6035 pz -3

6036 pz -4

6037 pz -5

6038 pz -6

6039 pz -7

6040 pz -8

6041 pz -9

6042 pz -10

6043 pz -11

6044 pz -12

6045 pz -13

6046 pz -14

6047 pz -15

6048 pz -16

6049 pz -17

6050 pz -18

6051 pz -19

6052 pz -20

6053 pz -21

6054 pz -22

6055 pz -23

6056 pz -24

6057 pz -25

6058 pz -26

6059 pz -27

6060 pz -28

6061 pz -29

6062 pz -30

6063 pz -31

6064 pz -32

6065 pz -33

6066 pz -34

6067 pz -35

6068 pz -36

7000 pz +30.861

7001 pz +27.305

7002 pz +25.781

7003 pz +22.225

7004 pz +20.701

7005 pz +17.145

7006 pz +15.621

7007 pz +12.065

7008 pz +10.541

7009 pz +6.985

7010 pz +5.461

7011 pz +1.905

7012 pz +0.381

7013 pz -3.175

7014 pz -4.699

7015 pz -8.255

7016 pz -9.779

7017 pz -13.335

7018 pz -14.859

7019 pz -18.415

7020 pz -19.939

7021 pz -23.495

7022 pz -25.019

7023 pz -28.575

7024 pz -30.099

7025 pz -33.655

7026 pz -35.179

c

8000 pz +30.7975 \$ Bottom of upper grid plate region

8001 pz +27.7368 \$ Top of graphite region

8002 pz +19.05 \$ Top of fuel region

8003 pz -19.05 \$ Bottom of fuel region

8004 pz -27.7368 \$ Bottom of graphite region

8005 pz -33.17875 \$ Top of lower grid plate region

c

c -----

c Tube surface for my test (Alex Zhou 2009)

c -----

9001 rcc +19.59102 +11.31062 0.05 0 0 1.5 0.5 \$sample space inside container

9002 rcc +19.59102 +11.31062 0 0 0 1.6 0.55 \$container of polyethylene

9003 c/z +19.59102 +11.31062 +1.816 \$ assembly for G34

9004 c/z +19.59102 +11.31062 +1.867 \$ out shell

c 9010 rcc +19.59102 +11.31062 -1.7 0 0 5 1.5 \$ surface source bound

c

c -----

c End of Surface Card Specification

c -----

c -----

c Beginning of Material Card Specification

c -----

c -----

c Beam tube transformations

c -----

c tr1: Through port, small, BP1

c tr2: Tangential port, small, BP2

c tr3: Radial port, large, BP3

c tr4: Radial port, small, BP4

c tr5: Through port, large, BP5

c

*tr1 0.0 -35.255 -6.985 00 90 90 90 00 90

*tr2 +35.255 -06.222 -6.985 30 120 90 60 30 90

*tr3 0.0 +25.600 -6.985 00 90 90 90 00 90

*tr4 -22.871 +13.216 -6.985 60 30 90 150 60 90

*tr5 0.0 -35.255 -6.985 00 90 90 90 00 90

c

c the '*' just makes the transformation in degrees

c

c -----

c Control rod transformations

c -----

c Shutdown condition -000 units

c Low power critical -525 units

c Design high power -700 units

c Full out condition -960 units

c

tr6 0 0 00.00 1 0 0 0 1 0

tr7 0 0 23.40 1 0 0 0 1 0 \$ Formerly 19.05, 8.33, 12.37

tr8 0 0 27.78 1 0 0 0 1 0

tr9 0 0 38.10 1 0 0 0 1 0

c

c -----

c Mapping experiment transformations

c -----

tr10 +2.17678 -1.2573 0.0

tr11 +15.23746 -1.2573 0.0

tr12 +19.59102 -1.2573 0.0

tr13 +23.94458 -1.2573 0.0

c

c -----

c Irradiation facility transformations

c -----

tr20 -15.23746 -8.79856 0.0 \$ Center of 3L irradiator

tr50 +15.23746 -11.31062 0.0 \$ Center of 6L irradiator

c

c -----

c Grid plate hole transformations

c -----

tr100 -0.00000 +0.00000 0.0 \$ A1

tr101 +4.35356 +0.00000 0.0 \$ B1

tr102 +2.17678 -3.76936 0.0 \$ B2

tr103 -2.17678 -3.76936 0.0 \$ B3

tr104 -4.35356 +0.00000 0.0 \$ B4

tr105 -2.17678 +3.76936 0.0 \$ B5

tr106 +2.17678 +3.76936 0.0 \$ B6

tr107 +8.70712 +0.00000 0.0 \$ C1

tr108 +6.53034 -3.76936 0.0 \$ C2

tr109 +4.35356 -7.54126 0.0 \$ C3

tr110 -0.00000 -7.54126 0.0 \$ C4

tr111 -4.35356 -7.54126 0.0 \$ C5

tr112 -6.53034 -3.76936 0.0 \$ C6

tr113 -8.70712 +0.00000 0.0 \$ C7
tr114 -6.53034 +3.76936 0.0 \$ C8
tr115 -4.35356 +7.54126 0.0 \$ C9
tr116 -0.00000 +7.54126 0.0 \$ C10
tr117 +4.35356 +7.54126 0.0 \$ C11
tr118 +6.53034 +3.76936 0.0 \$ C12
tr119 +13.06068 +0.00000 0.0 \$ D1
tr120 +10.88390 -3.76936 0.0 \$ D2
tr121 +8.70712 -7.54126 0.0 \$ D3
tr122 +6.53034 -11.31062 0.0 \$ D4
tr123 +2.17678 -11.31062 0.0 \$ D5
tr124 -2.17678 -11.31062 0.0 \$ D6
tr125 -6.53034 -11.31062 0.0 \$ D7
tr126 -8.70712 -7.54126 0.0 \$ D8
tr127 -10.88390 -3.76936 0.0 \$ D9
tr128 -13.06068 +0.00000 0.0 \$ D10
tr129 -10.88390 +3.76936 0.0 \$ D11
tr130 -8.70712 +7.54126 0.0 \$ D12
tr131 -6.53034 +11.31062 0.0 \$ D13
tr132 -2.17678 +11.31062 0.0 \$ D14
tr133 +2.17678 +11.31062 0.0 \$ D15
tr134 +6.53034 +11.31062 0.0 \$ D16
tr135 +8.70712 +7.54126 0.0 \$ D17
tr136 +10.88390 +3.76936 0.0 \$ D18
tr137 +17.41424 +0.00000 0.0 \$ E1
tr138 +15.23746 -3.76936 0.0 \$ E2
tr139 +13.06068 -7.54126 0.0 \$ E3

tr140 +10.88390 -11.31062 0.0 \$ E4
tr141 +8.70712 -15.08252 0.0 \$ E5
tr142 +4.35356 -15.08252 0.0 \$ E6
tr143 -0.00000 -15.08252 0.0 \$ E7
tr144 -4.35356 -15.08252 0.0 \$ E8
tr145 -8.70712 -15.08252 0.0 \$ E9
tr146 -10.88390 -11.31062 0.0 \$ E10
tr147 -13.06068 -7.54126 0.0 \$ E11
tr148 -15.23746 -3.76936 0.0 \$ E12
tr149 -17.41424 +0.00000 0.0 \$ E13
tr150 -15.23746 +3.76936 0.0 \$ E14
tr151 -13.06068 +7.54126 0.0 \$ E15
tr152 -10.88390 +11.31062 0.0 \$ E16
tr153 -8.70712 +15.08252 0.0 \$ E17
tr154 -4.35356 +15.08252 0.0 \$ E18
tr155 -0.00000 +15.08252 0.0 \$ E19
tr156 +4.35356 +15.08252 0.0 \$ E20
tr157 +8.70712 +15.08252 0.0 \$ E21
tr158 +10.88390 +11.31062 0.0 \$ E22
tr159 +13.06068 +7.54126 0.0 \$ E23
tr160 +15.23746 +3.76936 0.0 \$ E24
tr161 +21.76780 +0.00000 0.0 \$ F1
tr162 +19.59102 -3.76936 0.0 \$ F2
tr163 +17.41424 -7.54126 0.0 \$ F3
tr164 +15.23746 -11.31062 0.0 \$ F4
tr165 +13.06068 -15.08252 0.0 \$ F5
tr166 +10.88390 -18.85188 0.0 \$ F6

tr167 +6.53034 -18.85188 0.0 \$ F7
tr168 +2.17678 -18.85188 0.0 \$ F8
tr169 -2.17678 -18.85188 0.0 \$ F9
tr170 -6.53034 -18.85188 0.0 \$ F10
tr171 -10.88390 -18.85188 0.0 \$ F11
tr172 -13.06068 -15.08252 0.0 \$ F12
tr173 -15.23746 -11.31062 0.0 \$ F13
tr174 -17.41424 -7.54126 0.0 \$ F14
tr175 -19.59102 -3.76936 0.0 \$ F15
tr176 -21.76780 +0.00000 0.0 \$ F16
tr177 -19.59102 +3.76936 0.0 \$ F17
tr178 -17.41424 +7.54126 0.0 \$ F18
tr179 -15.23746 +11.31062 0.0 \$ F19
tr180 -13.06068 +15.08252 0.0 \$ F20
tr181 -10.88390 +18.85188 0.0 \$ F21
tr182 -6.53034 +18.85188 0.0 \$ F22
tr183 -2.17678 +18.85188 0.0 \$ F23
tr184 +2.17678 +18.85188 0.0 \$ F24
tr185 +6.53034 +18.85188 0.0 \$ F25
tr186 +10.88390 +18.85188 0.0 \$ F26
tr187 +13.06068 +15.08252 0.0 \$ F27
tr188 +15.23746 +11.31062 0.0 \$ F28
tr189 +17.41424 +7.54126 0.0 \$ F29
tr190 +19.59102 +3.76936 0.0 \$ F30
tr191 +23.94458 -3.76936 0.0 \$ G2
tr192 +21.76780 -7.54126 0.0 \$ G3
tr193 +19.59102 -11.31062 0.0 \$ G4

tr194 +17.41424 -15.08252 0.0 \$ G5
tr195 +15.23746 -18.85188 0.0 \$ G6
tr196 +8.70712 -22.62124 0.0 \$ G8
tr197 +4.35356 -22.62124 0.0 \$ G9
tr198 -0.00000 -22.62124 0.0 \$ G10
tr199 -4.35356 -22.62124 0.0 \$ G11
tr200 -8.70712 -22.62124 0.0 \$ G12
tr201 -15.23746 -18.85188 0.0 \$ G14
tr202 -17.41424 -15.08252 0.0 \$ G15
tr203 -19.59102 -11.31062 0.0 \$ G16
tr204 -21.76780 -7.54126 0.0 \$ G17
tr205 -23.94458 -3.76936 0.0 \$ G18
tr206 -23.94458 +3.76936 0.0 \$ G20
tr207 -21.76780 +7.54126 0.0 \$ G21
tr208 -19.59102 +11.31062 0.0 \$ G22
tr209 -17.41424 +15.08252 0.0 \$ G23
tr210 -15.23746 +18.85188 0.0 \$ G24
tr211 -8.70712 +22.62124 0.0 \$ G26
tr212 -4.35356 +22.62124 0.0 \$ G27
tr213 +4.35356 +22.62124 0.0 \$ G29
tr214 -0.00000 +22.62124 0.0 \$ G28
tr215 +8.70712 +22.62124 0.0 \$ G30
tr216 +15.23746 +18.85188 0.0 \$ G32
tr217 +17.41424 +15.08252 0.0 \$ G33
c tr218 +19.59102 +11.31062 0.0 \$ G34
tr219 +21.76780 +7.54126 0.0 \$ G35
tr220 +23.94458 +3.76936 0.0 \$ G36

c

c -----

c Reactor component materials

c -----

c m1 -water

c m2 -aluminum (structural) type 6061

c m3 -stainless steel (structural) type 304

c m4 -graphite (carbon)

c m5 -fresh U-ZrH fuel

c m6 -B₄C (boron carbide)

c m7 -zirconium (rod)

c m8 -air

c m10 -cadmium (neutron absorber liner)

c m11 -lead (neutron absorber liner)

c

m1 1001 0.66667

8016 0.33333

mt1 lwtr.60t

c mpn1 0 0

m2 13027 -0.9685

26000.50c -0.0070

29000.50c -0.0025

14000.60c -0.0060

12000.66c -0.0110

24000.50c -0.0035

25055 -0.0015

c

c mpn2 0 0 0 0 0 0 0

m3 26000.50c -0.6785

6000 -0.0080

14000.60c -0.0100

24000.50c -0.1800

28000.50c -0.0980

25055 -0.0180

15031 -0.0045

16000.66c -0.0030

c

c mpn3 0 0 0 0 0 0 0 0

c

m4 6000 1.0

mt4 grph.60t \$ 300K

c mpn4 0

c

m5 40090 -0.462589265

40091 -0.100879525

40092 -0.154196422

40094 -0.156264362

40096 -0.025174926

1001 -0.0158955

92238 -0.068170

92235 -0.016830

c

c mpn5 0 0 82208 82208

mt5 zr/h.60t

h/zr.60t

c

m6 5010 0.1584

5011 0.6416

6000 0.2

c

c mpn6 0 0 0

m7 40090 51.45

40091 11.22

40092 17.15

40094 17.38

40096 2.8

c

c mpn7 0

m8 8016 -0.23

7014 -0.77

c mpn8 0 0

m10 48000.42c 1.0

c mpn10 0

m11 82000.42c -1.0

c

c mpn11 0

m12 28058 1 \$ nickel (n,p) a/o 68.0

m13 28064 1 \$ nickel (n,g) a/o 0.9

m14 79197 1 \$ gold (n,g) a/o 100.0

m15 29063 1 \$ copper (n,g) a/o 69.1

m16 26058 1 \$ iron (n,g) a/o 0.2

m17 26054 1 \$ iron (n,p) a/o 5.8
m18 42098 1 \$ molybdenum (n,g) a/o 24.1
m19 27059 1 \$ cobalt (n,g) a/o 100.0
m20 13027 1 \$ aluminum (n,g) a/o 100.0
m21 14000.60c -0.005 \$ 1100 borated aluminum alloy
26000.50c -0.005
29000.50c -0.001
25055 -0.005
30000.42c -0.0001
5010 -0.04275
5011 -0.00225
13027 -0.9389

c

m22 26056 1 \$ Iron (n,p) a/o 91.754
m23 57139 1 \$ Lanthanum (n,g) a/o 99.9098
m24 73181 1 \$ Tantalum (n,g) a/o 99.988
m25 22047 1 \$ Titanium (n,p) a/o 7.44
m26 22048 1 \$ Titanium (n,p) a/o 73.72
m27 14030 1 \$ Silicon (n,x) a/o 3.1
m28 24050 1 \$ Chromium (n,x) a/o 4.345
m29 29065 1 \$ Copper (n,x) a/o 30.83
m30 50112 1 \$ Tin (n,x) a/o 0.97
m31 50116 1 \$ Tin (n,x) a/o 14.54
m32 50118 1 \$ Tin (n,x) a/o 24.22
m33 50122 1 \$ Tin (n,x) a/o 4.63
m34 50124 1 \$ Tin (n,x) a/o 5.79
m35 82204 1 \$ Lead (n,x) a/o 1.4

m36 82206 1 \$ Lead (n,x) a/o 24.1
m37 18040 1 \$ Argon (n,g) a/o 99.6003
m38 24052 1 \$ Chromium (n,p) a/o 83.789
m39 22050 1 \$ Titanium (n,g) a/o 5.18
m40 42100 1 \$ Molybdenum (n,g) a/o 9.63
m41 16032 1 \$ Sulfur-32 (n,p) a/o 95.02

c

c -----

c Tube material for my test (Alex Zhou 2009)

c -----

m99 1001 2

6012 1

MT99 POLY.60t \$ CH₂, polyethylene

m9910 1001 -.11111 \$.001% NaCl solution

8016 -.88888

11023 -3.93E-6

17000 -6.07E-6

m9911 1001 -.1111 \$.01% NaCl solution

8016 -.8888

11023 -3.93E-5

17000 -6.07E-5

m9912 1001 -.111 \$.1% NaCl solution

8016 -.888

11023 -3.93E-4

17000 -6.07E-4

m9913 1001 -.11 \$ 1% NaCl solution

8016 -.88

```

11023 -3.93E-3
17000 -6.07E-3
m9914 1001 -.1 $ 10% NaCl solution
8016 -.8
11023 -3.93E-2
17000 -6.07E-2
m9992 2001 .667
8016 .333
MT9992 hwtr.60c
m9993 11023 1 $ Na
m9994 17000 1 $ Cl
m9995 1001 1 $ H
m9996 1002 1 $ D
c
c -----
c Criticality calculation
c -----
c 10000 n/cycle, 1.000 as initial guess, skip 30, total of 60 keff cycles,
c automatic plotting of three combined keff tally
c
kcode 10000 1.000 30 60 4500 0 6500 1
mplot freq 10 kcode 16 scales 2
ksrc -4.5 21.8 13 0 21.8 13 4.5 21.8 13 -11 18 13
      -6.5 18.0 13 -2 18.0 13 2.0 18 13 6.5 18 13
      11 18 13 -17.5 14.3 13 -13 14.3 13 -9 14.3 13
      -4.5 14.3 13 0 14.3 13 4.5 14.3 13 9 14.3 13
      13 14.3 13 -19.5 10.5 13 -15.5 10.5 13 -11 10.5 13

```


-6.5 10.5 13 2 10.5 13 6.5 10.5 13 11 10.5 13
 15.5 10.5 13 19.5 10.5 13 -22 6.8 13 -17.5 6.8 13
 -13 6.8 13 -9 6.8 13 -4.5 6.8 13 0 6.8 13
 4.5 6.8 13 9 6.8 13 13 6.8 13 17.5 6.8 13
 -19.5 2.8 13 -15.5 2.8 13 -11 2.8 13 -6.5 2.8 13
 -2 2.8 13 2 2.8 13 6.5 2.8 13 11 2.8 13
 15.5 2.8 13 19.5 2.8 13 -22 -0.8 13 -17.5 -0.8 13
 -13 -0.8 13 -4.5 -0.8 13 4.5 -0.8 13 13 -0.8 13
 17.5 -0.8 13 22 -0.8 13 -24 -4.6 13 -19.5 -4.6 13
 -15.5 -4.6 13 -11 -4.6 13 -6.5 -4.6 13 -2 -4.6 13
 2 -4.6 13 6.5 -4.6 13 11 -4.6 13 15.5 -4.6 13
 19.5 -4.6 13 -22 -8.3 13 -9 -8.3 13 -4.5 -8.3 13
 0 -8.3 13 4.5 -8.3 13 9 -8.3 13 13 -8.3 13
 17.5 -8.3 13 22 -8.3 13 -11 -12 13 -6.5 -12 13
 2 -12 13 6.5 -12 13 11 -12 13 15.5 -12 13
 19.5 -12 13 -17.5 -15.9 13 -13 -15.9 13 -9 -15.9 13
 -4.5 -15.9 13 0 -15.9 13 4.5 -15.9 13 9 -15.9 13
 13 -15.9 13 17.5 -15.9 13 -15.5 -19.7 13 -11 -19.7 13
 -6.5 -19.7 13 -2 -19.7 13 2 -19.7 13 6.5 -19.7 13
 11 -19.7 13 -4.5 -23.5 13 0 -23.5 13 4.5 -23.5 13

c

thtme 0 \$ time in shakes (1e-8 sec) at which thermal temperatures...

mode n p

c phys:p 100 0 0 0 1 -102 \$ -102, Analog sampling, models only, multigroup + line emission

imp:n 1 314r 0

imp:p 1 314r 0

c F4:n 124

c energy band: thermal, epithermal, and fast

c ssW -9010 -111 121

E4 1E-6 1E-3 1

F7:n 124

F4:n 9001

FM4 (4.97e+7 9993 -1) (4.97e+7 9994 -1) (2.91e13 9995 -1)

FC4

print